THE ANTENNA LABORATORY

RESEARCH ACTIVITIES in ---

Automatic Controls *Antennas* *Echo Area Studies*
Microwave Circuits *Astronautics* *E M Field Theory*
Terrain Investigations *Radomes* *Systems Analysis*
Wave Propagation *Submillimeter Applications*

AN ANALYSIS OF ANTENNAS
CONFRONTED BY OBSTACLES

by

Thomas E. Charlton

Contract AF 33(616)-7614
Task Number 42039

1180-8 30 November 1961

Department of ELECTRICAL ENGINEERING

THE OHIO STATE UNIVERSITY
RESEARCH FOUNDATION
Columbus, Ohio

REPORT 1180-8

R E P O R T

by

THE OHIO STATE UNIVERSITY RESEARCH FOUNDATION
COLUMBUS 12, OHIO

Cooperator	Aeronautical Systems Division Air Force Systems Command United States Air Force Wright-Patterson Air Force Base Ohio
Contract	AF 33(616)-7614
Task Number	42039
Investigation of	Study of Electromagnetic Window Dielectric Techniques
Subject of Report	An Analysis of Antennas Confronted by Obstacles
Submitted by	Thomas E. Charlton Antenna Laboratory Department of Electrical Engineering
Date	30 November 1961

ACKNOWLEDGEMENTS

The author wishes to acknowledge the work of Professor J. H. Richmond, for much of this work is based upon his developments and refinements of the principle of reciprocity. Illuminating discussions with Professor Richmond and other members of the Antenna Laboratory were of valuable assistance, and the encouragement and help of J. R. Collier is also appreciated.

ABSTRACT

The principle of reciprocity is employed to formulate integral expressions for the fields of antennas confronted by obstacles. The expressions thus formulated are particularly useful in applying a high-speed computer to the calculation of antenna-obstacle interaction. The integrals encountered require surface integrations over the antenna aperture or on a surface enclosing the obstacle.

The problem of computing the far-field pattern of an antenna-obstacle system is treated in detail. These calculations can be completed by employing the antenna "aperture fields" and the plane wave fields scattered from the obstacle. An alternate method of calculation requires a knowledge of the fields set up on the obstacle by the antenna.

A number of approximate methods for finding the plane-wave scattered fields and the fields on the obstacles are discussed. Well-established techniques exist for obstacles very small or very large in terms of wavelength, but treatment of scatterers in the intermediate range, the resonance region, is more complex. The investigator must choose the method to fit the problem in order to proceed efficiently. For this reason, several different techniques are discussed which can be programmed for high speed computation.

The validity of the expressions formulated is checked by a comparison of experiment and calculation. The far-field principal-plane patterns of various horns in the presence of long cylinders were measured and calculated by means of these expressions. Excellent agreement is obtained even for cylinder-to-horn separations of only a few wavelengths. The calculations employ plane wave - infinite cylinder boundary value solutions and an integration over the antenna aperture.

More complex obstacle configurations, a cylinder and dielectric sheet combination, and finally a pair of parallel cylinders are treated successfully by approximate methods.

TABLE OF CONTENTS

	Page
CHAPTER I - INTRODUCTION	1
CHAPTER II - THE THEORETICAL FORMULATION OF THE ANTENNA-OBSTACLE PROBLEM	3
A. THE FORMULATION OF THE BASIC RELATION	3
B. THE FIELDS OF AN ANTENNA NEAR AN OBSTACLE	8
C. SOLVING FOR THE FIELDS	11
1. The antenna aperture fields	12
2. The fields on the surface S_s	14
3. The fields of J_2	16
4. The dipole moment of J_2	18
5. Evaluating the surface integrals	18
CHAPTER III - APPROXIMATE SOLUTIONS TO THE ANTENNA-OBSTACLE PROBLEM	20
A. GENERAL REMARKS	20
B. OBSTACLES SMALL IN TERMS OF WAVELENGTH	21
C. LARGE OBSTACLES	24
D. OBSTACLE GEOMETRIES IN THE RESONANCE REGION	27

Page

1. Iteration of the exact solution 28

2. Multipole expansion 30

3. Variational method 31

4. Approximate current method 33

CHAPTER IV - ANTENNAS CONFRONTED BY CYLINDERS 36

A. CYLINDRICAL OBSTACLES 36

B. BOUNDARY VALUE SOLUTION 37

1. Calculation 42

2. Experiment 44

C. RESULTS 45

1. The small horn and a cylinder 45

2. A horn confronted by a cylinder and dielectric sheet 51

3. A large ground plane antenna and a cylinder 57

4. Antenna confronted by a pair of parallel cylinders 59

CHAPTER V - CONCLUSIONS 62

APPENDIX A - THE EXTERNAL BOUNDARY INTEGRAL 65

	Page
APPENDIX B - THE APERTURE FIELD APPROXIMATION	66
APPENDIX C - ELIMINATION OF THE INTEGRAL OVER S_s	76
BIBLIOGRAPHY	80
AUTOBIOGRAPHY	86

CHAPTER I

INTRODUCTION

As the frontiers of space are expanded and the problems encountered in the fields of communication, guidance, detection and tracking become more complex due to increased velocities and new environments, the problems associated with antenna system design and analysis also become more complex. Antenna-obstacle interaction is such a problem.

The obstacle problem is becoming more acute with respect to the performance of high-speed vehicle antenna systems. Infrared systems, streamlined radomes, pitot static booms, radome supports, and other antennas, these all act as obstacles and affect antenna performance.

On the ground, the increased size of antennas for long-range communications necessitates the use of very large radomes and large antenna feeds. These and their associated supports act as obstacles.

This paper deals with the calculation of the effects of obstalces upon antenna system patterns. The formulation of a solution is made so that any extensive study of an obstacle or class of obstacles can be programmed on a high-speed computer.

Finally, an experimental and theoretical study of a number of antenna-obstacle systems is made. The results verify the theory and indicate that calculations are practical.

CHAPTER II

THE THEORETICAL FORMULATION OF THE ANTENNA-OBSTACLE PROBLEM

A. THE FORMULATION OF THE BASIC RELATION

The analysis of many phases of an electromagnetic problem can be completed by invoking the principle of reciprocity. In particular, when a scatterer is placed in the near field of an antenna system, expressions for such quantities as antenna gain, pattern, boresight direction, and impedance[1] can be formulated by use of the reciprocity theorems. The expressions thus deduced are in the form of surface or volume integrals. It has been shown[2] that a variety of integral expressions are available depending upon the surface chosen and the test source used. Thus that form of the solution to a given problem should be chosen which yields numerical results most readily. As the problem is formulated the shape and electrical properties of the scatterer as well as the size and illumination of the antenna will be seen to affect this choice.

The physical and mathematical significance of the "reaction" and reciprocity are well treated in the literature;[3,4] however, the theoretical formulation of the antenna-obstacle problem will be developed from fundamentals for the sake of clarity.

Consider an infinite, homogeneous, isotropic medium with the parameters μ_o and ϵ_o in which are located an antenna (a source of electromagnetic energy) and various scatterers (passive bodies with electrical properties differing from the infinite medium). Antenna 1 is located in a volume V_1 enclosed by the surface S_1, and all the scatterers are located in a different volume V_s enclosed by S_s. This is illustrated in Fig. 1.

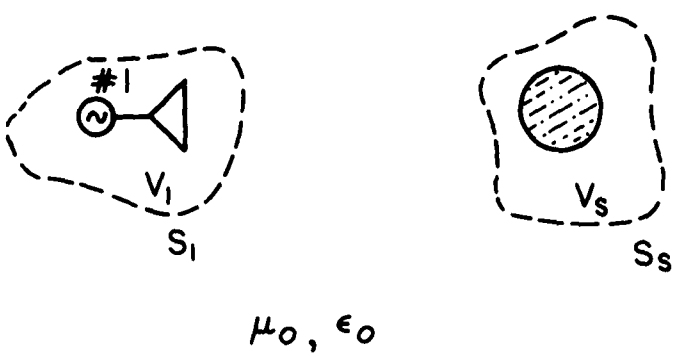

Fig. 1. Antenna 1 and the scatterer in free space.

The electromagnetic fields of any antenna in S_1 can be related by Maxwell's equations as follows:

(1) $$\nabla \times \underline{E}_1 = -j\omega\mu_1 \underline{H}_1 \ ,$$

and

(2) $$\nabla \times \underline{H}_1 = j\omega\epsilon_1 \underline{E}_1 + \underline{J}_1$$

In these equations and throughout this paper the fields are assumed to vary as $e^{j\omega t}$ with respect to time, and the current $\underline{J}_1$ depends upon the source located in V_1. Finally μ_1 and ϵ_1 can be replaced by μ_o and ϵ_o respectively everywhere outside of V_1 and V_s, while inside V_1 and V_s μ_1 and ϵ_1 depend upon the antenna and scatterers postulated. Thus for all regions outside V_1 and V_s the equations

$$\nabla \times \underline{E}_1 = -j\omega\mu_o \underline{H}_1 \tag{3}$$

and

$$\nabla \times \underline{H}_1 = j\omega\epsilon_o \underline{E}_1 \tag{4}$$

hold. The fields $\underline{E}_1$ and $\underline{H}_1$ are members of the set of all fields whose source is restricted to the volume V_1 and which exist in an infinite medium arbitrary only inside the volume V_s.

Consider next a second antenna (No. 2) located in a volume V_2 surrounded again by an infinite, homogeneous, isotropic medium (μ_o, ϵ_o) except the volume V_s which can contain any arbitrary passive bodies as illustrated in Fig. 2.

The electromagnetic fields of antenna 2 can be related by Maxwell's equations as follows,

$$\nabla \times \underline{E}_2 = -j\omega\mu_2 \underline{H}_2 \ , \tag{5}$$

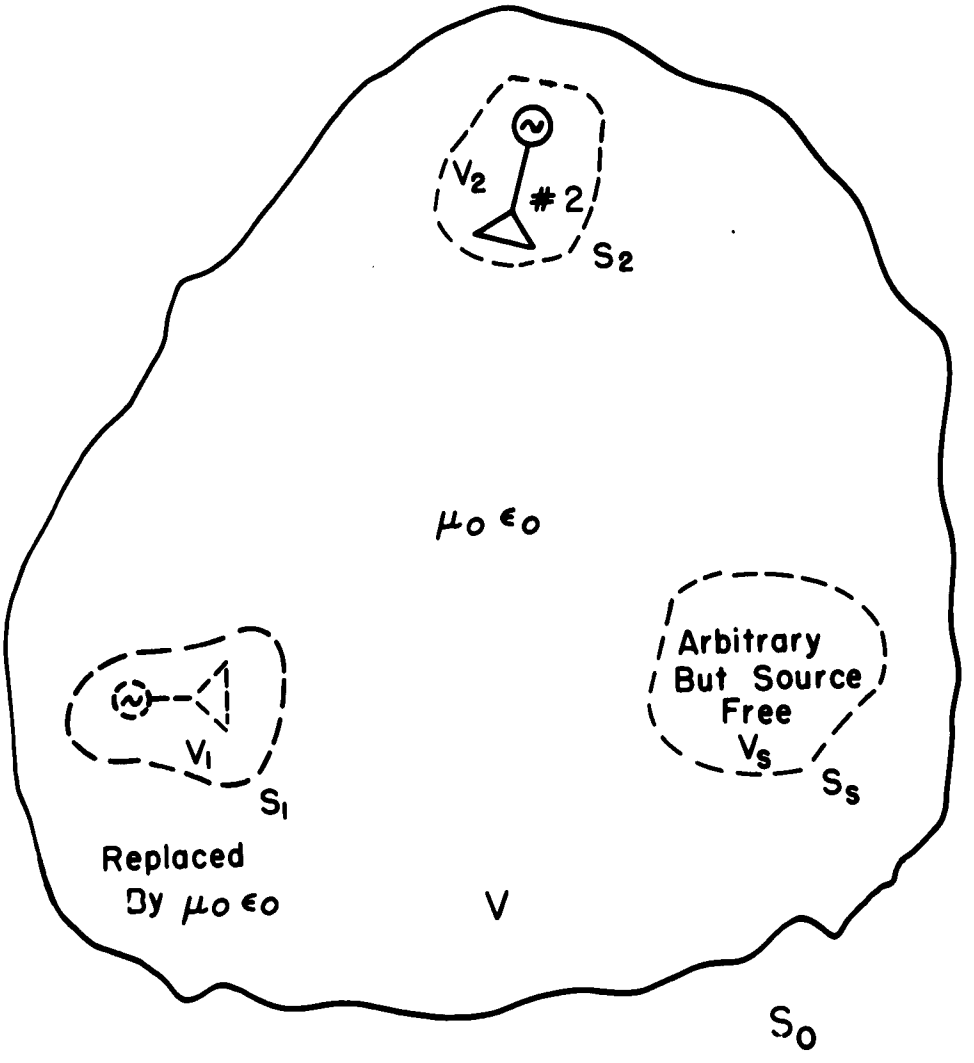

Fig. 2. Antenna 2 and the arbitrary volume V_s in free space.

(6) $$\nabla \times \underline{H}_2 = j\omega\epsilon_2 \underline{E}_2 + \underline{J}_2 ,$$

and outside of V_2 and V_s

(7) $$\nabla \times \underline{E}_2 = -j\omega\mu_o \underline{H}_2 ,$$

$$\nabla \times \underline{H}_2 = j\omega \epsilon_o \underline{E}_2 \quad . \tag{8}$$

The fields $\underline{E}_2$ and $\underline{H}_2$ are members of the set whose source is restricted to the volume V_2 and which exist in an infinite medium arbitrary only in a volume V_s.

By using relations (3), (4), (7) and (8) and the vector identity $\nabla \cdot (\underline{A} \times \underline{B}) = \underline{B} \cdot \nabla \times \underline{A} - \underline{A} \cdot \nabla \times \underline{B}$, it is found that

$$\nabla \cdot (\underline{E}_1 \times \underline{H}_2 - \underline{E}_2 \times \underline{H}_1) = 0 \tag{9}$$

everywhere exterior to V_1, V_2 and V_s. A volume integration of Eq. (9) over this exterior volume yields

$$\int_V \nabla \cdot (\underline{E}_1 \times \underline{H}_2 - \underline{E}_2 \times \underline{H}_1)\, dV = 0 \quad . \tag{10}$$

The divergence theorem can now be applied to Eq. (10) since the fields are well-behaved functions in and on the boundary of V. Thus

$$\int_V \nabla \cdot (\underline{E}_1 \times \underline{H}_2 - \underline{E}_2 \times \underline{H}_1)\, dV = \int_S (\underline{E}_1 \times \underline{H}_2 - \underline{E}_2 \times \underline{H}_1) \cdot \hat{n}\, dS = 0 \tag{11}$$

where S is the surface enclosing the volume V and $\hat{n}$ is the unit normal directed out of V. The surface S is composed of the internal boundaries S_1, S_2, and S_s and an external boundary S_o. Therefore

Eq. (11) can be rewritten as:

$$(12) \qquad \int_{S_1+S_2+S_s} (\underline{E}_1 \times \underline{H}_2 - \underline{E}_2 \times \underline{H}_1) \cdot \hat{n}\, dS + \int_{S_o} (\underline{E}_1 \times \underline{H}_2 - \underline{E}_2 \times \underline{H}_1) \cdot \hat{n}\, dS = 0 \ .$$

The external surface integral is discussed in Appendix A and does not contribute to Eq. (12) so that

$$(13) \qquad \int_{S_1} (\underline{E}_1 \times \underline{H}_2 - \underline{E}_2 \times \underline{H}_1) \cdot \hat{n} dS + \int_{S_s} (\underline{E}_1 \times \underline{H}_2 - \underline{E}_2 \times \underline{H}_1) \cdot \hat{n} dS$$

$$= \int_{S_2} (\underline{E}_2 \times \underline{H}_1 - \underline{E}_1 \times \underline{H}_2) \cdot \hat{n}\, dS \ .$$

This relation can now be used to solve many aspects of antenna-obstacle problems.

B. THE FIELDS OF AN ANTENNA NEAR AN OBSTACLE

Equation (13) can be used to compute the fields of an antenna transmitting in the presence of an obstacle. The fields $\underline{E}_1$ and $\underline{H}_1$ appearing in Eq. (13) are the fields of just such an antenna (See Fig. 1).

In order to find $\underline{E}_1$ at an arbitrary point in space (x_o, y_o, z_o), it is observed that within V_2

$$(14) \qquad \nabla \cdot (\underline{E}_1 \times \underline{H}_2 - \underline{E}_2 \times \underline{H}_1) = j\omega(\mu_2 - \mu_o)\underline{H}_1 \cdot \underline{H}_2 - j\omega(\epsilon_2 - \epsilon_o)\,\underline{E}_1 \cdot \underline{E}_2 - \underline{J}_2 \cdot \underline{E}_1 \quad .$$

Now let antenna 2 be an infinitesimal filament of electric current located at x_o, y_o, z_o with μ_2, $\epsilon_2 = \mu_o$, ϵ_o in V_2. Then

$$(15) \qquad \nabla \cdot (\underline{E}_1 \times \underline{H}_2 - \underline{E}_2 \times \underline{H}_1) = - \underline{J}_2 \cdot \underline{E}_1$$

in V_2 and

$$(16) \qquad \int_{V_2} \nabla \cdot (\underline{E}_1 \times \underline{H}_2 - \underline{E}_2 \times \underline{H}_1)\,dV = - \int_{V_2} \underline{J}_2 \cdot \underline{E}_1 \, dV \quad .$$

The divergence theorem yields

$$(17) \qquad \int_{S_2} (\underline{E}_1 \times \underline{H}_2 - \underline{E}_2 \times \underline{H}_1) \cdot \hat{n}\, dS = - \int_{V_2} \underline{J}_2 \cdot \underline{E}_1 \, dV \, ,$$

and since $\underline{J}_2$ is an infinitesimal current filament

$$(18) \qquad \int_{S_2} (\underline{E}_1 \times \underline{H}_2 - \underline{E}_2 \times \underline{H}_1) \cdot \hat{n}\, dS = -\underline{E}_1(x_o, y_o, z_o) \cdot \hat{\ell}_2 \; I_2$$

where I_2 and $\hat{\ell}_2$ describe the strength and orientation of $\underline{J}_2$ respectively. Finally, combining Eq. (13) and (18) yields

$$(19) \qquad \int_{S_1} (\underline{E}_1 \times \underline{H}_2 - \underline{E}_2 \times \underline{H}_1) \cdot \hat{n}\, dS + \int_{S_s} (\underline{E}_1 \times \underline{H}_2 - \underline{E}_2 \times \underline{H}_1) \cdot \hat{n}\, dS$$

$$= \underline{E}_1 (x_o, y_o, z_o) \cdot \hat{\ell}_2 \; I_2 \quad .$$

The unknown field $\underline{E}_1 (x_o, y_o, z_o)$ can thus be computed in terms of the above surface integrals when an infinitesimal electric current filament is used. The surface integrations are equivalent to a solution of the boundary value problem in that the necessary boundary conditions are imposed by specifying or knowing the fields $\hat{n} \times \underline{E}_1$ and $\hat{n} \times \underline{H}_1$ on the surfaces S_1 and S_s. The use of a current filament to formulate Eq. (19) is a modification of the work of Dr. J.H. Richmond.[2]

In solving Eq. (19) only the component of $\underline{E}_1$ parallel to the current is found; of course finding all three components of $\underline{E}_1$ simply amounts to the use of three mutually perpendicular dipoles. Finally, other quantities of interest, such as antenna gain, pattern, etc., are found by examining the form of $\underline{E}_1 (x_o, y_o, z_o)$.

C. SOLVING FOR THE FIELDS

The result of the previous section, namely Eq. (19), permits a solution for the fields of an arbitrary antenna in the presence of an obstacle provided that

1. the fields $\underline{E}_1$ and $\underline{H}_1$ are known on S_1 in the presence of the obstacle;
2. the fields $\underline{E}_1$, $\underline{H}_1$, $\underline{E}_2$ and $\underline{H}_2$ are known on the surface S_s;
3. the fields $\underline{E}_2$ and $\underline{H}_2$ of an electric current filament at (x_o, y_o, z_o) are known on S_1 when radiating into an environment arbitrary within the volume V_s but free space elsewhere;
4. the dipole moment, $\int_{V_2} J_2 \, dV = \hat{\ell}_2 \, I_2$, is known when the current radiates into this environment;
5. and the surface integrals over S_1 and S_s can be evaluated in closed form or by numerical techniques.

It is appropriate to discuss each of these provisions in more detail.

1. The antenna aperture fields. The fields $\underline{E}_1$ and $\underline{H}_1$ on some surface, S_1, enclosing the antenna under investigation are referred to as the "aperture fields" of the antenna. In order to employ Eq. (19) and compute the far field of the antenna these aperture fields must be known.

During free space operation the aperture fields are assumed known through measurement, design, or previous theoretical investigation. The free-space aperture fields thus constitute the starting point for finding the aperture fields in the presence of the obstacle.

The fields $\underline{E}_1$ and $\underline{H}_1$ on S_1 certainly depend upon the environment exterior to S_1 and thus can be expected to differ markedly not only when an obstacle is introduced but when it is reoriented or relocated.

The free-space field of the antenna is incident upon the obstacle and is scattered. This scattered field then is incident upon the antenna structure and is rescattered. This process of reflection and rereflection continues ad infinitum. Thus, the fields $\underline{E}_1$ and $\underline{H}_1$ of an antenna-obstacle system consist of:

1. the free-space fields of the antenna,

2. the fields scattered from the obstacle,

3. and the fields scattered from the antenna structure.

Richmond[5] has shown that the second of these, the fields scattered from the obstacle, do not contribute to the integration on S_1 in Eq. (19).

In Appendix B the contribution of the fields scattered from the antenna structure to this integration is discussed. A particular antenna-obstacle geometry is treated which points out the factors that affect the magnitude of the error introduced by neglecting this contribution. Such an approximation amounts to using the free-space aperture fields in evaluating the integral on S_1 in Eq. (19).

The experimental and calculated results of Chapter IV and the discussion in Appendix B indicate that such an approximation is very accurate except when:

1. the antenna and obstacle are very close together (separation less than 4λ for horn and cylinder),
2. the obstacle is near the focal point of an antenna system or near a large plane reflector,
3. or the antenna input is poorly matched.

2. The fields on the surface S_s. In order to evaluate the surface integral over S_s in Eq. (19) the fields $\underline{E}_1$, $\underline{E}_2$, $\underline{H}_1$ and $\underline{H}_2$ must be known on S_s. In general these fields are unknown on that surface, although in particular cases their measurement could be justified. Theoretical evaluation of $\underline{E}_1$ and $\underline{H}_1$ on S_s constitutes a problem that is as difficult as solving the antenna-obstacle problem itself, since it is a solution of that same problem on a designated surface.

It is fortunate that there exists a particular choice for the environment within V_s of the current filament $\underline{J}_2$ that causes the integration over S_s to vanish. This is discussed in Appendix C, and it will suffice here to say that by employing the fields of $\underline{J}_2$ in the presence of the same obstacle as for the antenna under investigation, the integral vanishes and Eq. (19) becomes

$$\int_{S_1} (\underline{E}_1 \times \underline{H}_2 - \underline{E}_2 \times \underline{H}_1) \cdot \hat{n}\, dS = \underline{E}_1(x_o, y_o, z_o) \cdot \hat{\ell}_2\, I_2 \quad . \tag{20}$$

A second possibility, of particular value when the free-space field, $\underline{E}_1^o$, is known, permits a calculation of the field scattered from the obstacle, $\underline{E}_1^s$, by an integration over the scattering surface S_s. In order to show this Eq. (20) is rewritten as

$$(21) \qquad \int_{S_1} (\underline{E}_1 \times \underline{H}_2 - \underline{E}_2 \times \underline{H}_1) \cdot \hat{n}\, dS = (\underline{E}_1^o + \underline{E}_1^s) \cdot \hat{\ell}_2\, I_2$$

and Eq. (19) can be written as

$$(22) \qquad \int_{S_1} (\underline{E}_1^o \times \underline{H}_2 - \underline{E}_2 \times \underline{H}_1^o) \cdot \hat{n}\, dS + \int_{S_s} (\underline{E}_1^o \times \underline{H}_2 - \underline{E}_2 \times \underline{H}_1^o) \cdot \hat{n}\, dS = \underline{E}_1^o \cdot \hat{\ell}_2\, I_2 \quad .$$

Based on the discussion of the antenna aperture fields in the last section, it is true for many antenna-obstacle geometries that

$$(23) \qquad \int_{S_1} (\underline{E}_1 \times \underline{H}_2 - \underline{E}_2 \times \underline{H}_1) \cdot \hat{n}\, dS = \int (\underline{E}_1^o \times \underline{H}_2 - \underline{E}_2 \times \underline{H}_1^o) \cdot \hat{n}\, dS \, .$$

Therefore combining Eq. (21), (22), and (23) yields

$$(24) \qquad \int_{S_s} (\underline{E}_1^o \times \underline{H}_2 - \underline{E}_2 \times \underline{H}_1^o) \cdot \hat{n}\, dS = - \underline{E}_1^s \cdot \hat{\ell}_2\, I_2$$

and by a similar reasoning process

$$(25) \qquad \int_{S_s} (\underline{E}_1 \times \underline{H}_2^o - \underline{E}_2^o \times \underline{H}_1) \cdot \hat{n}\, dS = \underline{E}_1^s \cdot \hat{\ell}_2\, I_2 \quad .$$

3. The fields of $\underline{J}_2$. As has already been shown it is convenient to postulate a current filament located at (x_o, y_o, z_o) in order to calculate the electric field at that point due to an antenna-obstacle system. Furthermore, application of Eq. (20) results in a solution when the fields of $\underline{J}_2$ in the presence of the scatterer are employed. From this equation it is seen that the fields $\underline{E}_2$ and $\underline{H}_2$ must be known on a surface enclosing the antenna of interest (S_1).

In order to evaluate these fields, it is helpful to examine the fields of a current $\underline{J}$ identical with $\underline{J}_2$ but radiating into free space. Such a current, when oriented as in Fig. 3, produces the fields

$$\underline{H} = \frac{J}{4\pi} \sin\theta \frac{e^{-jk_o r}}{r} \left[\frac{1}{r} + jk_o\right] \hat{\phi} \tag{26}$$

and

$$\underline{E} = \frac{\nabla \times \underline{H}}{j\omega\epsilon_o} = \frac{J}{4\pi\epsilon_o} \frac{e^{-jk_o r}}{r}$$

$$\left[\hat{\theta}\sin\theta\left(jk_o\sqrt{\mu_o\epsilon_o} + \frac{\sqrt{\mu_o\epsilon_o}}{r} + \frac{1}{j\omega r^2}\right)\right.$$

$$\left. + \hat{r}\, 2\cos\theta\left(\frac{\sqrt{\mu_o\epsilon_o}}{r} + \frac{1}{j\omega r^2}\right)\right] . \tag{27}$$

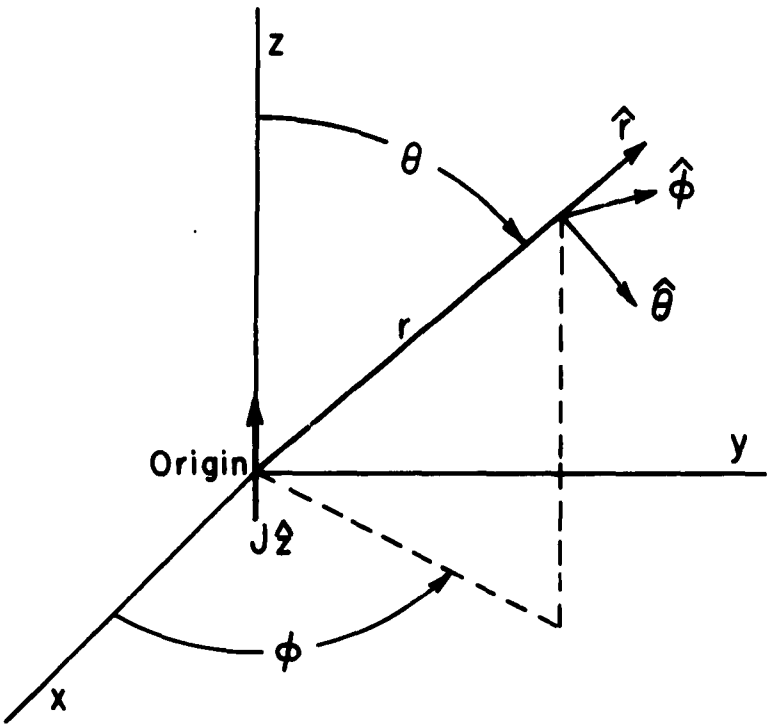

Fig. 3. The current J and its associated coordinate system.

As r becomes very large ($r >> \lambda_o$),

$$\underline{H} \cong \frac{J}{4\pi} \frac{jk_o \sin\theta\, e^{-jk_o r}}{r} \hat{\phi}\,, \tag{28}$$

$$\underline{E} \cong \frac{J}{4\pi} \frac{jk_o \sin\theta\, e^{-jk_o r}}{r} \sqrt{\frac{\mu_o}{\epsilon_o}}\, \hat{\theta}\,, \tag{29}$$

and

$$\underline{E} \cong -\hat{r} \times \underline{H} \sqrt{\frac{\mu_o}{\epsilon_o}} = -\hat{r} \times \underline{H}\, Z_o\,, \tag{30}$$

so that phase fronts propagate in a direction normal to $\underline{E}$ and $\underline{H}$ and the field vectors are perpendicular and related by the free space impedance, Z_o, in any small region of space.

Thus if a current $\underline{J}_2$ is a great distance from the obstacle, a solution to the plane wave scattering problem will yield $\underline{E}_2$ and $\underline{H}_2$. Here then is the utility of Eq. (20) — that the plane wave solutions to scattering problems can be used to calculate the far fields of antenna-obstacle systems.

4. The dipole moment of $\underline{J}_2$. The current filament, $\underline{J}_2$, was postulated mathematically and thus need not be physically realizable. It is possible to further postulate that the value of the dipole moment, $\int_{V_2} \underline{J}_2 \, dV = \hat{\ell}_2 \, I_2$, is fixed and does not depend upon environment or location. Such a current filament corresponds to an infinitesimal electric dipole fed by an infinitesimal constant current generator.

5. Evaluating the surface integrals. The formulation of integral expressions, such as Eq. (20), (24) and (25) for the field of an antenna-obstacle system, has been completed, so that numerical computations are possible. The possibility of evaluating the integrals in closed form exists, but in many practical cases the

aperture fields are known from measurement or design, so that numerical integration is more appropriate. The use of high-speed computers makes numerical techniques even more feasible for solving specific problems.

Finally, as demonstrated in later sections, proper choice of integration surfaces simplifies the calculations considerably.

CHAPTER III

APPROXIMATE SOLUTIONS TO THE ANTENNA-OBSTACLE PROBLEM

A. GENERAL REMARKS

In Chapter II a number of distinct integral expressions are derived for the field of an antenna in the presence of an obstacle, Eqs. (19), (20), (24) and (25). These are by no means the only possible expressions for the fields, but they are adequate for the present discussion. There are a few general remarks to be made before going into the details of solution.

First, the existence of high-speed digital computers and their tremendous capabilities allow the investigator to use numerical techniques on a large class of problems heretofore impractical. The integrals encountered in this antenna-obstacle study are members of this class.

Second, the choice of which expression to employ in solving a particular problem ultimately is determined by an estimate of the calculation time of each.

Finally, the integral expressions deduced to facilitate calculation of antenna-obstacle patterns require a knowledge of either the plane-wave scattering of the obstacle, Eqs. (20) and (24), or the

tangential fields induced by the antenna on the scattering surface, Eq. (25). Solving for these quantities becomes the greatest problem to overcome.

Exact boundary value solutions have been obtained for some obstacle geometries. The best known of these are the sphere and the circular cylinder of infinite length. Expressions are available for the plane-wave scattering of such obstacles, but in many instances their usefulness for numerical calculation is limited because the infinite series encountered converge slowly. Thus any useful treatment of antenna-obstacle interaction which is applicable to analysis of an arbitrary obstacle must consider approximate techniques for evaluating these fields.

B. OBSTACLES SMALL IN TERMS OF WAVELENGTH

Lord Rayleigh[6] treated the problem of electromagnetic waves incident upon small obstacles before 1900. The success of his work is attested by the fact that scattering from bodies much smaller than a wavelength in cross section is today called "Rayleigh scattering". His method consists in viewing the incident field as uniform in the vicinity of the obstacle at any instant of time. Thus an electric and magnetic charge distribution on the scatterer can be computed by

employing the techniques of static electricity and magnetism. The harmonic nature of the fields then causes a small obstacle to scatter as equivalent electric and magnetic dipoles. The strength of these dipoles depends upon the values of the incident fields and the electrical and geometrical properties of the body. Thus

$$\underline{p}_e = \begin{pmatrix} a_{11} & a_{12} & a_{13} \\ a_{21} & a_{22} & a_{23} \\ a_{31} & a_{32} & a_{33} \end{pmatrix} \cdot \underline{E}^i(r_o) = \overset{\approx}{a} \cdot \underline{E}^i(r_o) \tag{31}$$

and

$$\underline{p}_m = \begin{pmatrix} b_{11} & b_{12} & b_{13} \\ b_{21} & b_{22} & b_{23} \\ b_{31} & b_{32} & b_{33} \end{pmatrix} \cdot \underline{H}^i(r_o) = \overset{\approx}{b} \cdot \underline{H}^i(r_o) \tag{32}$$

where $\underline{p}_e$ symbolizes an electric dipole and $\underline{p}_m$ a magnetic dipole, $\underline{H}^i(r_o)$ and $\underline{E}^i(r_o)$ are the incident fields at the center (of mass) of the body, and $\overset{\approx}{a}$ and $\overset{\approx}{b}$ are dyadics depending upon the geometric and electrical properties of the small obstacle.

In order to compute the fields of an antenna system in the presence of such a scatterer, use of Eq. (25) appears most practical. This means that the antenna near-field in free space must be given or computed at the obstacle location. Such a calculation is, at most, time-consuming when the aperture fields of the

antenna are known; the large the aperture, the longer the calculation time. The scattered field of the equivalent dipoles Eq. (31) and Eq. (32) can then be found by means of Eq. (25). Finally the fields of the antenna-obstacle system are given by the sum of the free-space antenna fields and these scattered fields. Again, the free-space antenna fields at most involve a lengthy calculation, but this can be readily programmed.

A second approximate approach to interaction between antennas and very small obstacles is the use of volume polarization currents.[7] This technique is useful because the scattered fields from a dielectric body can be thought of as originating from a volume distribution of electric and magnetic current radiating into free space. These currents occupy the dielectric volume and are given by

(33) $$\underline{J}_p = j\omega (\epsilon - \epsilon_o) \underline{E}$$

and

(34) $$\underline{K}_p = j\omega (\mu - \mu_o) \underline{H} ,$$

where μ and ϵ are the parameters of the dielectric obstacle. In general $\underline{E}$ and $\underline{H}$, the fields inside the dielectric, are unknown.

However, for small dielectric bodies whose electrical properties (permittivity ϵ and permeability μ) differ only slightly from free space, these fields can be approximated by the incident field. Thus

$$\underline{J}_p \cong j\omega(\epsilon-\epsilon_o)\,\underline{E}^i \tag{35}$$

and

$$\underline{K}_p \cong j\omega\,(\mu-\mu_o)\,\underline{H}^i \quad . \tag{36}$$

The size of such an obstacle again makes Eq. (25) the most practical approach to calculating antenna-obstacle interaction.

The polarization current approach is limited to dielectric bodies which differ only slightly from free space but does offer an advantage in that it is applicable to a greater range of obstacle sizes, even to those normally thought of as lying in the resonance region.

C. LARGE OBSTACLES

The most common large obstacle encountered in antenna system design and analysis is the radome. In general, the exact solution for a plane wave incident upon an infinite homogeneous plane sheet can be used in conjunction with Eq. (20) to calculate the antenna pattern. Such an approach is approximate in that any physical radome is of finite size and in most cases is not plane.

This plane wave-plane sheet approximation gives useful results in all but the most streamlined radome problems. In such cases ray tracing can be attempted in the region of greatest curvature or the excitation of surface waves postulated as in the case of a wedge radome.[8] Richmond[9] has shown good agreement between measurement and calculation for an antenna aperture only partially obstructed by a dielectric sheet. The calculations are made by integrating on the surface of the sheet, i.e., Eq. (24) is used.

The analysis of inhomogeneous radomes as well as antennas surrounded by plasmas can be handled by means of plane wave theory and Eq. (20). The difficulty here stems from the complexity of the problem of a plane wave incident on an inhomogeneous plane sheet. Recent work by Richmond[10,11] provides efficient numerical techniques for calculating transmission and reflection coefficients as well as the fields inside such inhomogeneous layers.

In order to compute antenna-obstacle interaction for large conducting obstacles with large radii of curvature, physical optics is used. Physical optics consists of a special approximation of the current induced on the surface of a perfectly conducting obstacle.

In the shadow region the induced current is assumed to be zero while on the illuminated portion it is assumed to be

$$\underline{J} = 2\hat{n} \times \underline{H}^i \quad , \tag{37}$$

where $\hat{n}$ is the unit normal to the surface and $\underline{H}^i$ is the incident magnetic field. Such a current would indeed exist on an infinite plane conductor with unit normal $\hat{n}$.

In order to make use of this physical optics approximation while calculating the electric field of an antenna-obstacle system, it is most appropriate to employ Eq. (25). The free-space magnetic field of the antenna is first computed on a surface corresponding to that of the obstacle. The physical optics current, $\underline{J}$, set up by this field is then used in Eq. (25) to compute the scattered pattern.

A less known approximate technique which stems from the equivalence principle[12] yields an expression for an equivalent magnetic current on the illuminated surface,

$$\underline{K} = 2\,\underline{E}^i \times \hat{n} \quad , \tag{38}$$

and zero on the shadow portion. This approximation is subject to the same limitations on obstacle size and shape as is the physical optics approximation. A comparison of the two techniques is made by Harrington[13] and it is shown that the approximations are of the

same order. Thus, in general, the scattering as described by $\underline{K}$ is as close to the exact value as that given by the physical optics current $\underline{J}$.

D. OBSTACLE GEOMETRIES IN THE RESONANCE REGION

A class of obstacles exists for which neither large nor small obstacle approximations are at all successful. The surfaces of these bodies are characterized by regions of small or medium radii of curvature and their circumference is on the order of one to ten wavelengths.

The approximate techniques discussed in the last two sections are so successful in solving the large and small obstacle problems that emphasis in recent years has been upon developing methods for such "resonant region" geometries. The researcher thus has a choice of the methods developed by numerous physicists, engineers, and mathematicians in this area. Unfortunately, a solution by any of these methods usually requires an overwhelming amount of numerical work. For this reason the discussion of approximate techniques in the resonance region is limited in the following pages to those methods most readily programmed on high-speed computers.

1. Iteration of the exact solution. In principle any electromagnetic scattering problem can be solved by means of the boundary conditions and solutions to the wave equation. However, the wave equation is separable in only a few coordinate systems[14,15] and the surface of the scatterer does not always coincide with one of these coordinate surfaces. On the other hand, the straightforward nature of the boundary value solution and the knowledge that an exact solution can be formulated are good reasons for considering this method.

Employing a complete set of solutions to the wave equation and applying the boundary conditions yields equations for the unknown coefficients of this set. Whenever the scattering surface is a complete coordinate surface in which the wave equation is separable, e.g., sphere, infinite cylinder, infinite plane, etc., the boundary conditions and the orthogonality of this set of solutions serve to determine the unknown coefficients, and the problem is solved. Scatterers that are not complete coordinate surfaces yield an infinite system of equations in an infinite number of unknown constants (e.g., slotted cylinder,[16] conducting strips,[17] etc.).

Such systems of equations, although impractical for hand calculation, can be solved approximately on high-speed computers.

Often the infinite system of equations can be approximated successfully by a finite set.[18] The number of equations and unknowns needed to yield a good approximate solution depends upon the size and shape of the scatterer. The ability of high-speed computers to handle matrix problems and employ iterative techniques is the reason that this approach can be successful.

This method can be applied directly to the antenna-obstacle problem in either of two ways. First, the plane wave scattering from an obstacle is calculated by choosing $\underline{E}^i$ and $\underline{H}^i$ as plane wave fields, the resultant scattered fields ($\underline{E}_2$, $\underline{H}_2$) can then be used in the antenna aperture integration of Eq. (20). This method offers the advantage that many different antennas can be analyzed using the same scattering information. In order to compute a complete antenna-obstacle pattern this method becomes complex, for the scattering information must be known for plane waves incident from many different directions.

An alternative method is to compute the fields scattered from the obstacle using the antenna near field as the incident field. The scattered fields of the antenna-obstacle system are then given by Eq. (25). The disadvantage in this technique is that the whole procedure must be repeated for each new antenna encountered.

2. Multipole expansion. Recent work by Kennaugh[19] discusses a technique applicable to scatterers of finite surface area. The method is of particular value in computing the approximate scattered fields of bodies in the resonance region.

The completeness of the characteristic solutions to the wave equation in spherical coordinates makes it possible to write the fields scattered by any body in the form of an infinite series of spherical vector wave functions; one expansion is necessary in the interior of the scatterer while another is necessary in the external region. A solution to the problem involves an infinite number of unknown constants.

Rather than using iterative techniques, Kennaugh approximates the scattered field by a finite series of N characteristic solutions to the wave equation in spherical coordinates. This multipole expansion is then made to fit the boundary conditions at M points on the surface. The fit of the boundary conditions is made by minimizing the squared error of the tangential electric and magnetic fields at the M points. This makes it possible to choose any number of points at which to enforce the boundary conditions.

The flexibility and systematic nature of this technique makes it appealing, especially for use in conjunction with a high-speed computer. It is limited in that the accuracy of the approximate solution is unknown for most problems. However, the accuracy does depend upon the size of the body, the number of points chosen and their location.

The method originally proposed by Kennaugh involved minimizing the integral of the squared error over the surface of the scatterer. This technique, although more difficult to program, offers the advantage that for some scatterers the set of constants associated with the multipole expansion are identical with the exact values and are independent of the number of multipoles employed.

Consideration of how to compute antenna-obstacle interaction employing the results of this technique closely parallels the discussion in the last section. However, the investigator's control of the form of the scattered fields, i.e., the multipole expansion, would often make the antenna aperture integration, Eq. (20), the most practical method.

3. Variational method. The variational method consists in first finding a stationary expression for the quantity of interest in terms of another quantity related to the problem. Relating this to

the problem under discussion means that a stationary expression for the scattered field must be found in terms of the tangential fields on the surface of the scatterer.

Such a stationary expression has the property that a first order perturbation of the expressions for the tangential fields results in a second order change in the scattered field. The second order change is small if the tangential fields are close to the correct value. This property in turn means that the investigation can approximate the unknown tangential fields by known functions of arbitrary amplitude, C_n. These constants can be determined from the condition that

$$\frac{\partial |E^s|}{\partial C_n} = 0 \tag{39}$$

for all n when $|E^s|$ is stationary.

In order to make use of a high-speed computer the variational procedure must be carried out systematically. A zero-order calculation is made with a zero-order trial function and then, by adding higher-order trial functions, higher-order calculations are made until successive calculations yield the same result. The spherical wave functions are appropriate as the various order trial functions for nearly spherical scatterers while the cylindrical wave functions apply in the case of a long, thin body.

The non-mathematically inclined often experience difficulty in formulating the stationary expression. Rumsey[20] has introduced a quantity called the "reaction" which, when understood, yields stationary expressions more readily to the investigator. The reaction concept gives physical significance to the quantities involved and insight as to why the approximation is stationary.

4. Approximate current method. Many of the resonant region problems involve perfectly conducting scatterers. In such cases the scattered fields are easily found when the current flowing on the scatterer is known. Thus approximate techniques for finding this current have been studied in detail both experimentally and theoretically.

V.A. Fock[21] pioneered in the area of formulating an expression for the current induced by a plane wave on a perfect conductor. His work concentrated on two dimensional problems such as a plane wave incident normally on a circular or elliptic cylinder. He formulated an expression for the current in the region of the shadow boundary by replacing this portion of the surface with a parabola and then reasoned from physical considerations that the wave equation could be approximated by a simplified differential equation. The current computed for TE polarization by this method

compares favorably with the theoretical and experimental values in the region of the shadow boundary for cylinder diameters greater than a wavelength. The method has been extended to three dimensional problems and to TM fields by Goodrich.[22]

The exact expression for the current induced by a plane wave on a circular cylinder of infinite length is well known but is written as an infinite series. For cylinders of radius greater than a wavelength the series converges slowly so that extensive work has been done in obtaining asymptotic formulas for the current. Wetzel[23] and others[24] make use of the asymptotic form of the Hankel function and thus obtain expressions identical with Fock's for the current on a circular cylinder in the region of the shadow boundary. This formula also gives agreement in the deep shadow region, and by a higher order approximation of the Hankel function Wetzel's work handles even small cylinders. The result of computing the current on elliptic cylinders in terms of the radius of curvature at a point and the corresponding current on a circular cylinder of that radius has met with success.[25]

The formula of Fock and the asymptotic formulas of other investigators can be given physical significance which in turn aids in the investigation of other problems. The currents on cylinders

and spheres can be considered as decaying waves which travel around the conducting surface even into the deep shadow region. An enlightening discussion of this subject is given by King and Wu.[26]

A method applicable to dielectric bodies as well as to perfect conductors has been developed by Keller.[27] This method hinges on the concept of diffracted rays and the formulation of a geometric theory of diffraction. The diffracted rays are shown to obey a stationary principle (Fermat's principle for reflected and refracted rays). The biggest problem associated with this method is its adaptation to a high-speed digital computer program.

Recent work at The Ohio State University Antenna Laboratory by Peters and Thomas[28] indicates progress on the problem of scattering from dielectric bodies in the resonance region. Their method is based upon geometric optics and gives good results for backscatter from dielectric spheres.

CHAPTER IV

ANTENNAS CONFRONTED BY CYLINDERS

A. CYLINDRICAL OBSTACLES

One of the most common obstructions encountered in antenna design is the cylinder. The feeds of large reflectors are often supported by metal cylinders, refueling and instrumentation booms upset the performance of systems located in the nose of aircraft and missiles, and recent studies[29] of metal space frames for radome support indicate that metal cylinders may become an integral part of hypersonic vehicle antenna systems. These uses as well as the mathematical and geometrical simplicity of the cylinder make it an ideal starting point for antenna-obstacle calculations.

The results of previous sections indicate that the fields of an antenna-obstacle system can be found by

1. finding the fields of $\underline{J}_2$ on the appropriate surface,
2. deducing the aperture fields of the antenna, and
3. performing the integration indicated in Eq.(20) or (24).

The second and third of these steps vary little from problem to problem and in most cases only consume a great deal of calculation time. The first step can be completed either in an exact manner or by the approximate techniques discussed in Chapter III.

B. BOUNDARY VALUE SOLUTION

In order to apply Eq. (20) the fields of the current filament, $\underline{J}_z$, must be known when it radiates in the presence of the obstacle. These fields can be deduced by considering a plane wave of appropriate amplitude and phase incident upon the obstacle when the obstacle and current are very far apart, as discussed in Chapter II. Such a solution yields the far field of an antenna-obstacle system and is the goal of this portion of the paper.

The solution for a plane wave incident upon a conducting right-circular cylinder is well known[30] and will not be derived here. The coordinate system and geometry are shown in Fig. 4. For an incident TE plane wave from a direction θ_o, ϕ_o the fields, in cylindrical coordinates, external to the cylinder are

$$E_z = 0 \tag{40}$$

$$E_\rho = E_z \left(\frac{-j}{\rho\, k_o \sin\theta_o}\right) \sum_{n=1}^{\infty} 2j^n n \left[J_n(k_o\rho \sin\theta_o) + C_n H_n^{(2)}(k_o\rho \sin\theta_o)\right] \sin n(\phi-\phi_o)\, e^{jk_o z \cos\theta_o} , \tag{41}$$

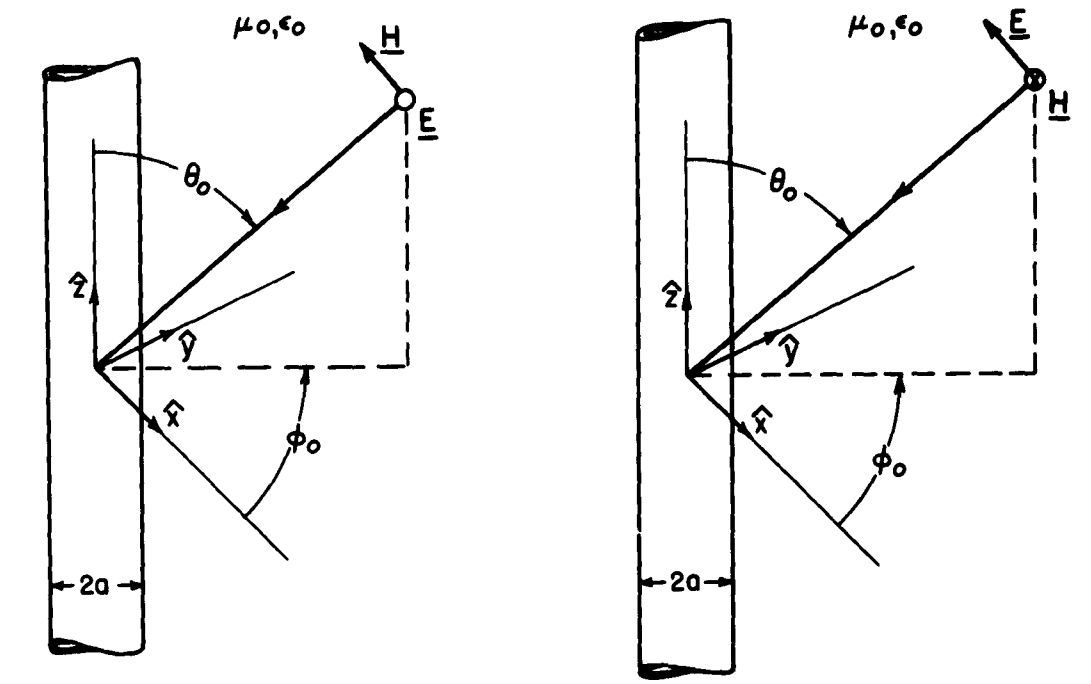

a) TE Polarization
($E_z = 0$)

b) TM Polarization
($H_z = 0$)

Fig. 4. TE and TM circular cylinders.

$$(42) \qquad E_\phi = E_2 (-j) \sum_{n=0}^{\infty} e_n j^n \left[J_n'(k_o \rho \sin\theta_o) + C_n H_n^{(2)\prime} (k_o \rho \sin\theta_o) \right] \cos n(\phi - \phi_o)\, e^{jk_o z \cos\theta_o} ,$$

$$(43) \qquad H_z = -\frac{E_2}{Z_o} \sum_{n=0}^{\infty} e_n j^n \left[J_n(k_o \rho \sin\theta_o) + C_n H_n^{(2)}(k_o \rho \sin\theta_o) \right] \cos n(\phi - \phi_o)\, e^{jk_o z \cos\theta_o} ,$$

$$(44) \qquad H_\rho = \frac{E_2}{Z_o} (-j \cos\theta_o) \sum_{n=0}^{\infty} e_n j^n \left[J_n'(k_o \rho \sin\theta_o) + C_n H_n^{(2)\prime} (k_o \rho \sin\theta_o) \right] \cos n(\phi - \phi_o)\, e^{jk_o z \cos\theta_o} ,$$

and

$$(45) \qquad H_\phi = \frac{E_2}{Z_o} \frac{j \cos\theta_o}{k_o \sin\theta_o} \sum_{n=1}^{\infty} 2j^n \left[J_n(k_o \rho \sin\theta_o) + C_n H_n^{(2)}(k_o \rho \sin\theta_o) \right] \sin n(\phi - \phi_o)\, e^{jk_o z \cos\theta_o} .$$

In these expressions E_2 is the magnitude of the plane wave, the primes indicate derivatives with respect to argument and $e_n = 1$ for $n = 0$, $e_n = 2$ for $n = 1, 2, 3 \cdots$. If the cylinder is a perfect

conductor of radius a, the constants C_n are given by

$$C_n = \frac{-J_n'(k_o a \sin\theta_o)}{H_n^{(2)\prime}(k_o a \sin\theta_o)} \quad . \tag{46}$$

If the cylinder is composed of homogeneous, isotropic dielectric material (μ_r, ϵ_r) of radius a, and the plane wave is incident normally, $\theta_o = \pi/2$, the constants C_n are given by[31]

$$C_n = \frac{\sqrt{\epsilon_r}\, J_n(k_o a) J_n'(k_o a\sqrt{\mu_r\epsilon_r}) - \sqrt{\mu_r}\, J_n(k_o a\sqrt{\mu_r\epsilon_r})\, J_n'(k_o a)}{\sqrt{\mu_r}\, J_n(k_o a\sqrt{\mu_r\epsilon_r}) H_n^{(2)\prime}(k_o a) - \sqrt{\epsilon_r}\, J_n'(k_o a\sqrt{\mu_r\epsilon_r}) H_n^{(2)}(k_o a)} \quad . \tag{47}$$

Similarly for a TM incident plane wave,

$$H_z = 0 \tag{48}$$

$$H_\rho = \frac{E_2}{Z_o}\left(\frac{j}{\rho k_o \sin\theta_o}\right) \sum_{n=1}^{\infty} 2nj^n \left[J_n(k_o\rho \sin\theta_o) + D_n H_n^{(2)}(k_o\rho \sin\theta_o)\right] \sin n(\phi-\phi_o)\, e^{jk_o z\cos\theta_o} \quad , \tag{49}$$

$$H_\phi = \frac{E_2}{Z_o}(j) \sum_{n=0}^{\infty} e_n j^n \left[J_n'(k_o\rho \sin\theta_o) + D_n H_n^{(2)\prime}(k_o\rho \sin\theta_o)\right] \cos n(\phi-\phi_o)\, e^{jk_o z\cos\theta_o} \quad , \tag{50}$$

$$(51) \qquad E_z = -E_z \sum_{n=0}^{\infty} e_n j^n \left[J_n(k_o \rho \sin\theta_o) + D_n H_n^{(2)}(k_o \rho \sin\theta_o) \right] \cos n(\phi - \phi_o)\, e^{jk_o z \cos\theta_o},$$

$$(52) \qquad E_\rho = E_z \left(-j \cos\theta_o\right) \sum_{n=0}^{\infty} e_n j^n \left[J_n'(k_o \rho \sin\theta_o) + D_n H_n'^{(2)}(k_o \rho \sin\theta_o) \right] \cos n(\phi - \phi_o)\, e^{jk_o z \cos\theta_o},$$

and

$$(53) \qquad E_\phi = \frac{E_z\, j \cos\theta_o}{\rho\, k_o \sin\theta_o} \sum_{n=1}^{\infty} 2n j^n \left[J_n(k_o \rho \sin\theta_o) + D_n H_n^{(2)}(k_o \rho \sin\theta_o) \right] \sin n(\phi - \phi_o)\, e^{jk_o z \cos\theta_o}.$$

If the cylinder is a perfect conductor of radius a,

$$(54) \qquad D_n = \frac{-J_n(k_o a \sin\theta_o)}{H_n^{(2)}(k_o a \sin\theta_o)} .$$

If the cylinder is composed of homogeneous, isotropic dielectric (μ_r, ϵ_r) of radius a, and the wave is incident normally

$$(55) \qquad D_n = \frac{\sqrt{\mu_r}\, J_n(k_o a) J_n'(k_o a \sqrt{\mu_r \epsilon_r}) - \sqrt{\epsilon_r}\, J_n(k_o a \sqrt{\mu_r \epsilon_r}) J_n'(k_o a)}{\sqrt{\epsilon_r}\, H_n^{(2)}(k_o a) J_n(k_o a \sqrt{\mu_r \epsilon_r}) - \sqrt{\mu_r}\, J_n'(k_o a \sqrt{\mu_r \epsilon_r}) H_n^{(2)}(k_o a)} .$$

The above TE and TM expressions constitute a complete solution of plane wave scattering by conducting cylinders; any incident plane wave can be expressed as a linear combination of TE and TM plane waves. Moreover, plane wave scattering by dielectric coated metal cylinders as well as by concentric dielectric cylinders is given by these same expressions when the appropriate form of C_n and D_n is used[32] (found by satisfying the boundary conditions on the cylindrical surfaces and restricted to normal incidence).

Equations (40) through (55) yield the fields $\underline{E}_2$ and $\underline{H}_2$ necessary for evaluating the integral of Eq. (20). The performance of antennas confronted by cylinders was studied by calculating and measuring the patterns of antenna-cylinder combinations.

1. Calculation. As has been indicated the calculations were made employing Eq.(20) which requires an integration over the antenna aperture. Equation (20) was used rather than Eq. (24) or (25) for several reasons. First, Eqs. (24) and (25) involve integrating over the surface of the obstacle and for infinite or very long cylinders this was not desirable. Second, the calculations and measurements were carried out upon a number of different antennas for which good estimates of aperture fields were available.

The calculation of the plane-wave scattered fields over the antenna aperture was first carried out by approximating the appropriate infinite series, Eqs. (40) through (55), by a finite number of terms. For the cylinder diameters used, $d < 2\lambda$, ten terms of the series were found sufficient. The number of terms needed to calculate the scattered fields suggested a second method of calculation; the asymptotic form of the Hankel functions was employed, simplifying the series. This asymptotic approximation is

$$H_n^{(2)}(k_o\rho \sin\theta_o) \approx \frac{e^{-jk_o\rho \sin\theta_o}}{\sqrt{k_o\rho \sin\theta_o}} \left[e^{j\left(\frac{2n+1}{4}\pi\right)}\right] \sqrt{\frac{2}{\pi}} \tag{56}$$

for $k_o\rho \sin\theta_o >> 1$, and $k_o\rho \sin\theta_o >> n$. The successful use of Eq. (56) thus depends upon the distance between the antennas and cylinder, $\rho \sin\theta_o$. Use of Eq. (56) also depends upon the diameter of the cylinder which established the number, n, of significant terms necessary to evaluate the series.

The asymptotic approximation yields the bi-static scattered pattern of the cylinder. This has been programmed at The Ohio State University Antenna Laboratory and was used for some of the calculations.

The aperture integration of Eq. (20) was carried out on a desk calculator. Simpson's rule was employed and an estimate of the error was obtained graphically so that a sufficiently small increment would be chosen. Experimental measurement served as the final check of the accuracy of solution.

2. Experiment. All of the antenna-obstacle measurements were made indoors. The antenna-cylinder system was mounted on a turntable and rotated about a vertical axis. Antenna patterns were recorded on a logarithmic recorder which was driven synchronously with the turntable. A crystal detector(1N53) operating in the square-law region measured the received signal at the antenna terminals.

The overall length of the range was thirty feet and the frequency was 35 kmc (λ = 0.338 inches). These figures limited the size of the systems measured for which reliable far-field results could be observed. Antenna diameters greater than twenty wavelengths or antenna-cylinder spacings exceeding twenty wavelengths were not considered for this reason.

Finally finite lengths of metal and dielectric cylinders were used to approximate the infinite cylinders for which the calculations

were made. The cylinders were long enough so that a change in length caused no noticeable change in the measured patterns.

C. RESULTS

1. The small horn and a cylinder. The first step taken in obtaining a comparison between theory and experiment was the measurement of the free-space E and H plane patterns of the antenna. The assumed aperture fields were used in Eq. (20) to compute these free-space patterns. Measurement and calculation were then compared to test the accuracy of the aperture field assumption.

A one and one-half wavelength square horn fed by rectangular waveguide excited in the TE_{01} mode was the first antenna so tested. Results of the free-space measurements and calculations appear in Figs. 5 and 6. The phase of the aperture fields was computed using the apex of the horn as a phase center while the amplitude distribution was assumed to be that of the TE_{01} mode. The close agreement with experiment indicated that these assumptions were appropriate.

The aperture fields and the plane wave fields scattered from cylinders were then used to calculate the patterns of this antenna confronted by a perfectly conducting cylinder. The diameter of the

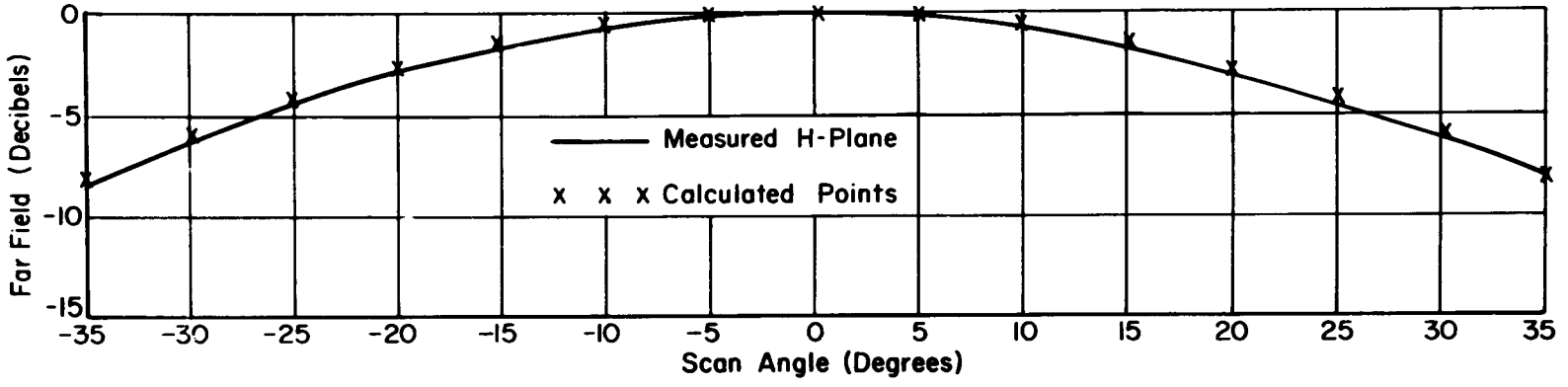

Fig. 5. The measured and calculated H plane pattern of the 1.5λ horn.

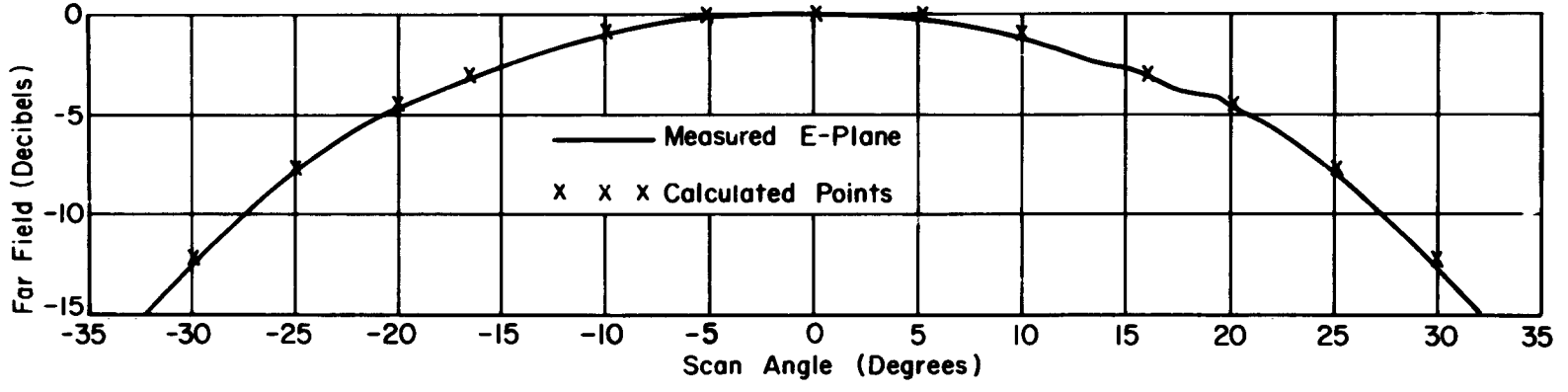

Fig. 6. The measured and calculated E plane pattern of the 1.5λ horn.

cylinder was chosen to be the same as the width of the antenna ($d = 1.5\lambda$). H plane measurements were made with the axis of the cylinder perpendicular to the plane of measurement, as shown in Fig. 7. In Figs. 7 through 10 the H plane patterns of the one and one-half wavelength horn are shown as the antenna-cylinder spacing was varied from four and one-half wavelengths to twelve wavelengths. The close agreement illustrated further attests to the validity of the aperture field assumptions.

The cylinder was reoriented so that the axis was perpendicular to the E plane as shown in Fig. 11 and an E plane measurement was made employing the one and one-half wavelength horn. Measurement and calculation are compared in Fig. 11; the agreement again is excellent. Finally a dielectric cylinder was introduced into the near field of the horn and an H plane measurement was made. The cylinder axis was perpendicular to the H plane, the diameter of the cylinder was one and one-half wavelengths and the dielectric constant two, $\epsilon_r = 2.0$. A comparison of calculation and experiment appears in Fig. 12.

These comparisions of measurement and calculation served to establish the validity of Eq. (20). The hand calculations were lengthy but not impractical.

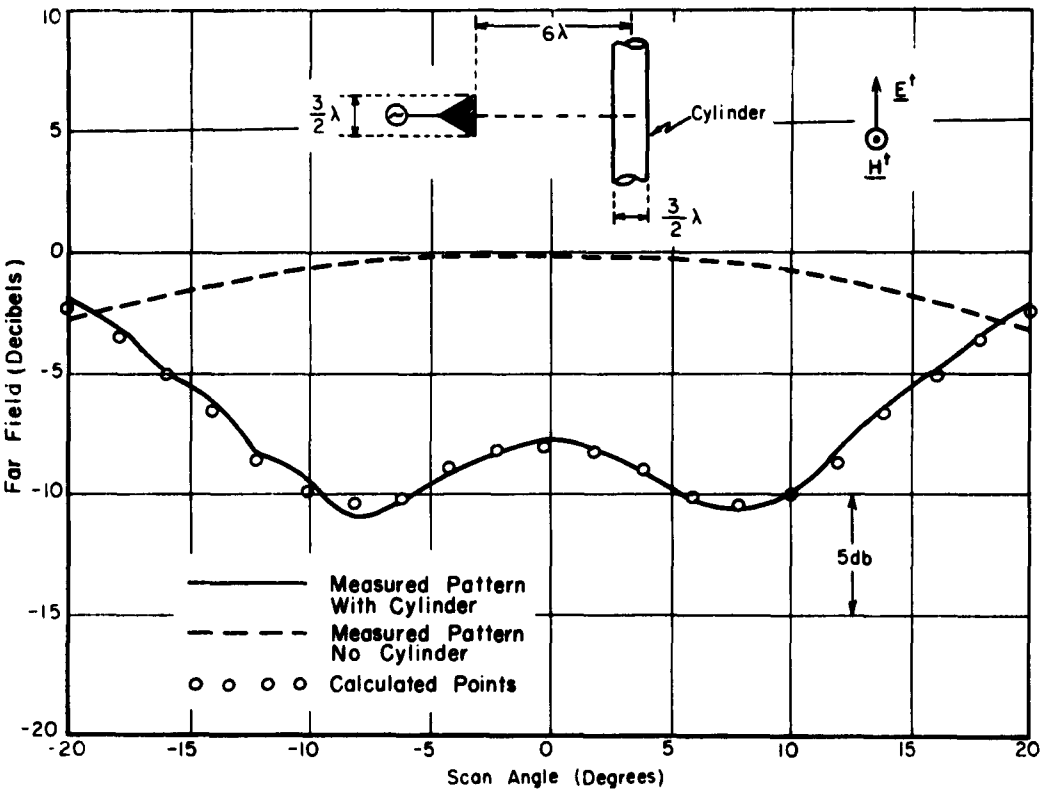

Fig. 7. The H plane pattern of the 1.5λ horn confronted by a 1.5λ cylinder at a distance of 6λ.

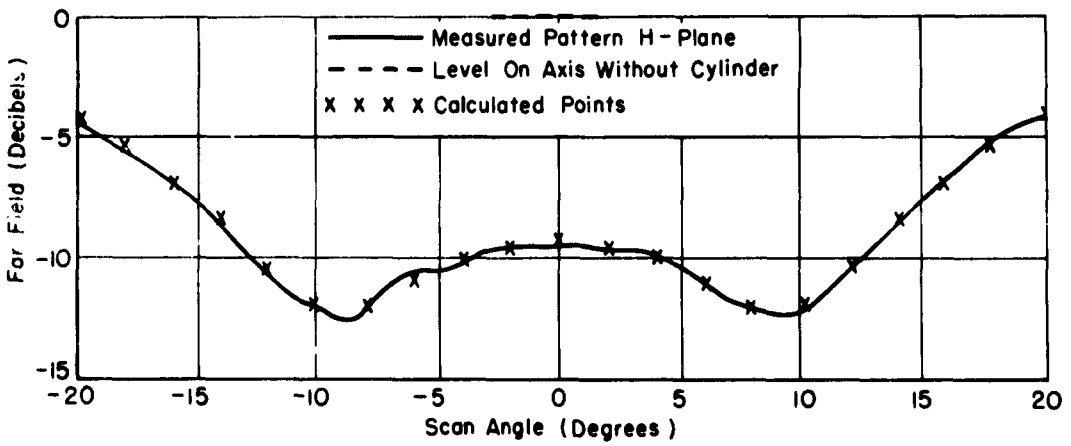

Fig. 8. The H plane pattern of the 1.5λ horn confronted by a 1.5λ cylinder at a distance of 4.5λ.

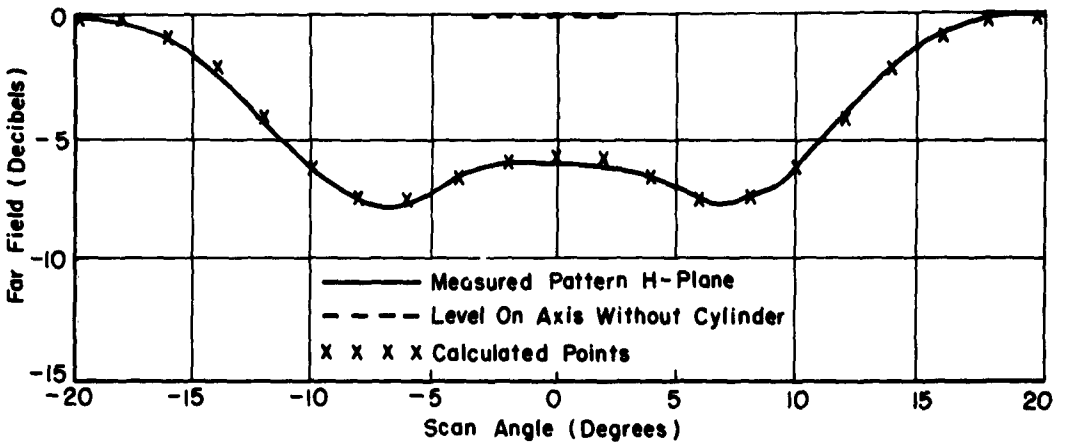

Fig. 9. The H plane pattern of the 1.5λ horn confronted by a 1.5λ cylinder at a distance of 9λ.

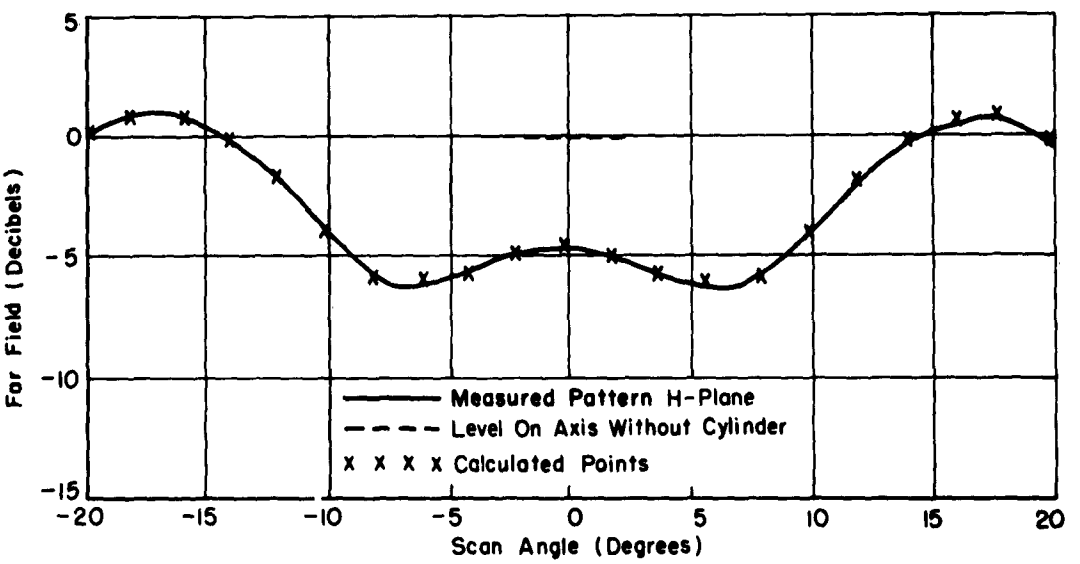

Fig. 10. The H plane pattern of the 1.5λ horn confronted by a 1.5λ cylinder at a distance of 12λ.

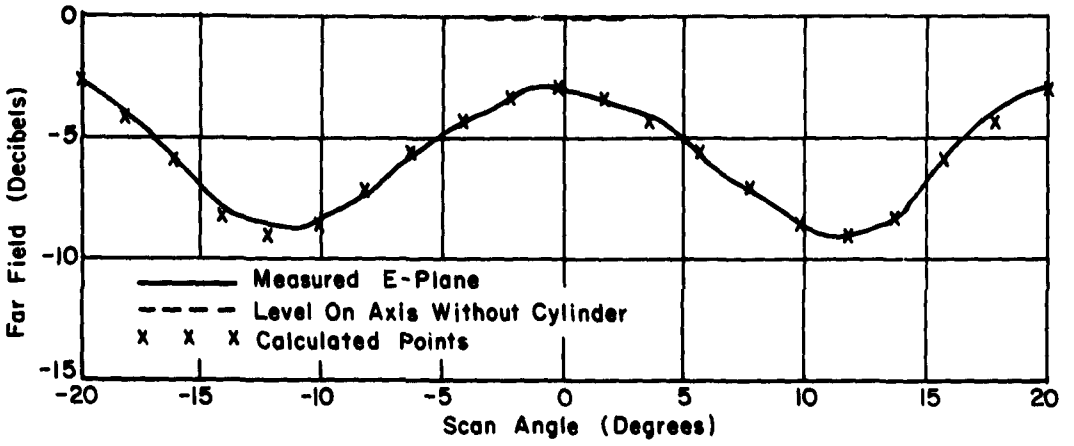

Fig. 11. The E plane pattern of the 1.5λ horn confronted by a 1.5λ cylinder at a distance of 6λ.

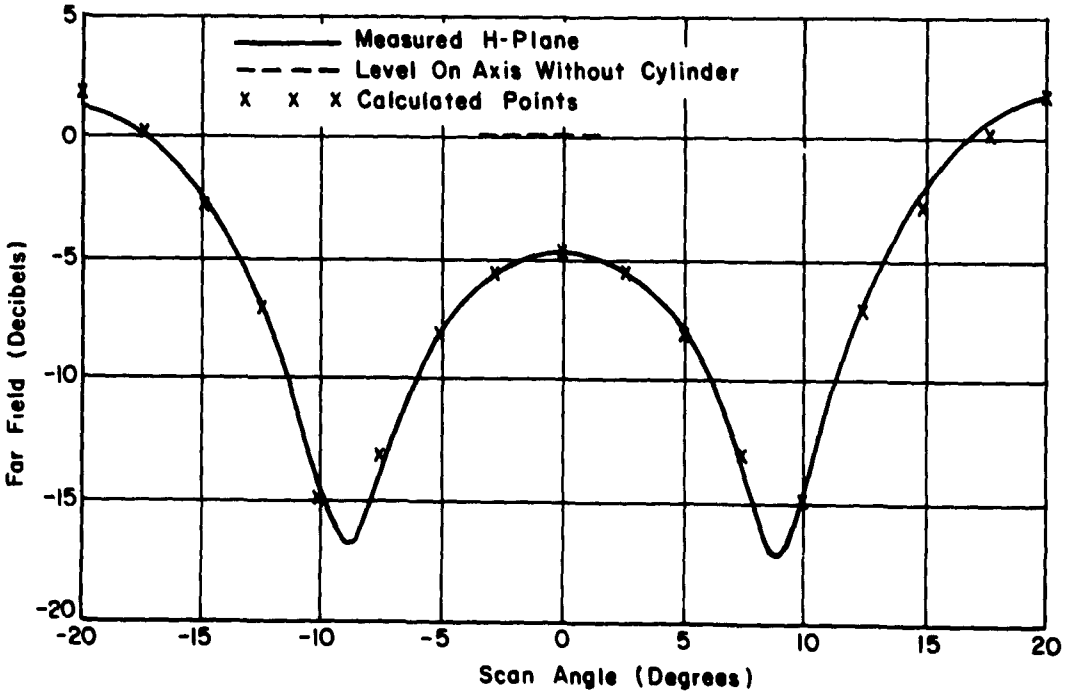

Fig. 12. The H plane pattern of the 1.5λ horn confronted by a 1.5λ dielectric ($\epsilon_r = 2.0$) cylinder at 6λ.

2. A horn confronted by a cylinder and dielectric sheet. Further work was done using a five wavelength square horn fed by the TE_{01} rectangular waveguide mode. A phase-correcting lens was used in the horn aperture designed to yield a constant phase distribution. The first step in making antenna-obstacle calculations employing this antenna again was a comparison of measured and calculated free space performance, Fig. 13. A constant-phase TE_{01} amplitude distribution yielded the calculated pattern, which closely approximated that measured.

The first antenna-obstacle system treated consisted of the perfectly conducting cylinder ($d = 1.5\lambda$) oriented perpendicular to the H plane, six wavelengths from the antenna. The measured and calculated H plane pattern appears in Fig. 14. The error present at the minima of this pattern is attributed to phase error present in the free-space aperture fields of the antenna.

A plane dielectric sheet ($d = 0.97\lambda$ and $\epsilon_r = 3.9$) was added to this antenna-cylinder configuration as shown in Fig. 15 and measurements were taken as the sheet was moved with respect to both the antenna and cylinder. These measurements appear in Figs. 15 thru 19. Figure 15 corresponds to the case of the sheet tangent to the side

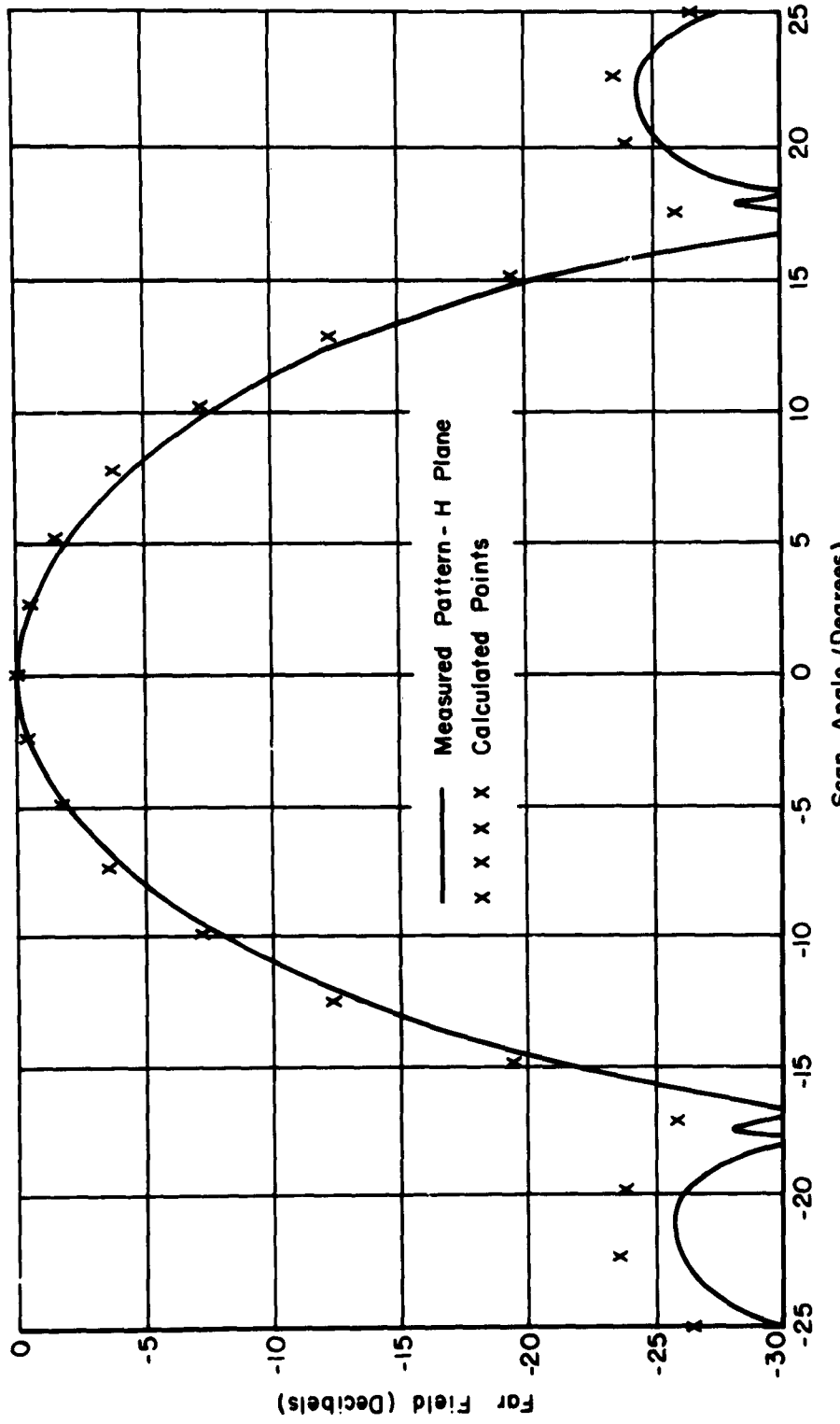

Fig. 13. The measured and calculated H plane pattern of the 5λ horn.

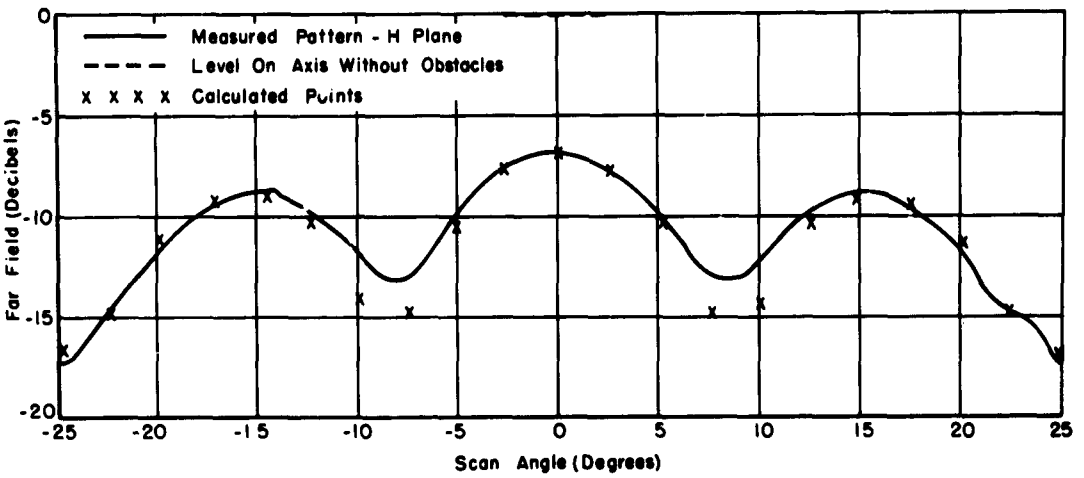

Fig. 14. The H plane pattern of the 5λ horn confronted by a 1.5λ cylinder at a distance of 6λ.

of the cylinder farthest from the antenna while Fig. 16 corresponds to the case of the sheet tangent to the side of the cylinder nearest the antenna.

In order to calculate the H-plane pattern of such a system an approximate approach was used to deduce the plane-wave scattered fields of the cylinder-sheet combination. These fields were then used in Eq. (20) to calculate the antenna pattern.

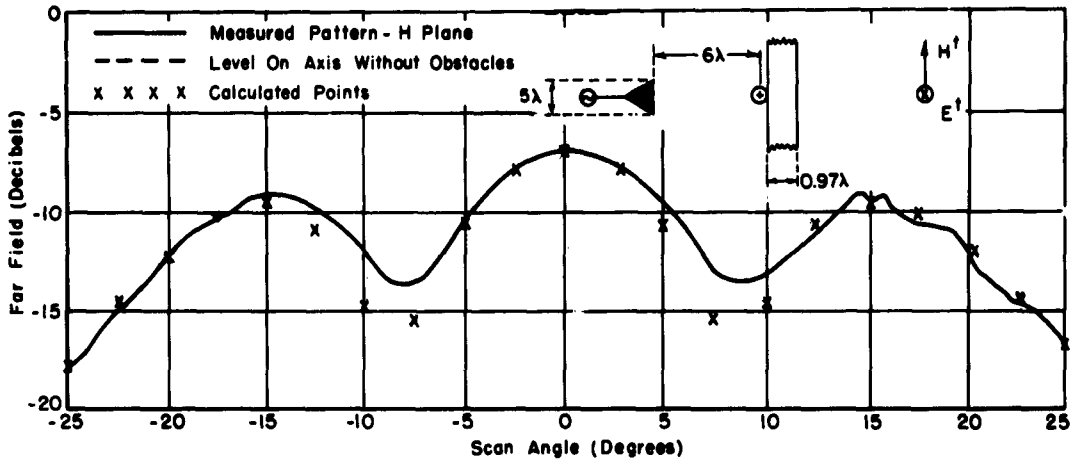

Fig. 15. The 5λ horn confronted by a 1.5λ cylinder at 6λ and dielectric sheet ($\epsilon_r = 3.9$, $d = 0.97\lambda$) at 6.75λ.

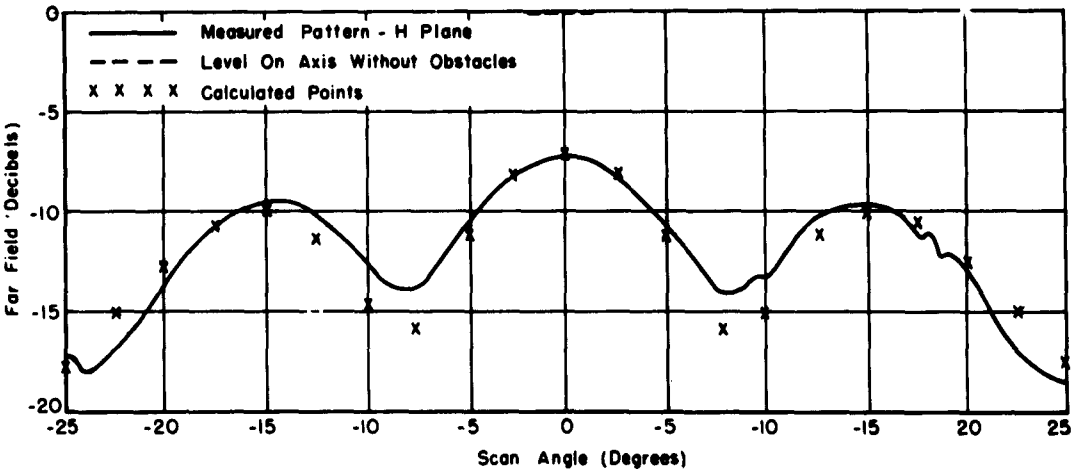

Fig. 16. The 5λ horn confronted by a 1.5λ cylinder at 6λ and dielectric sheet at 4.30λ.

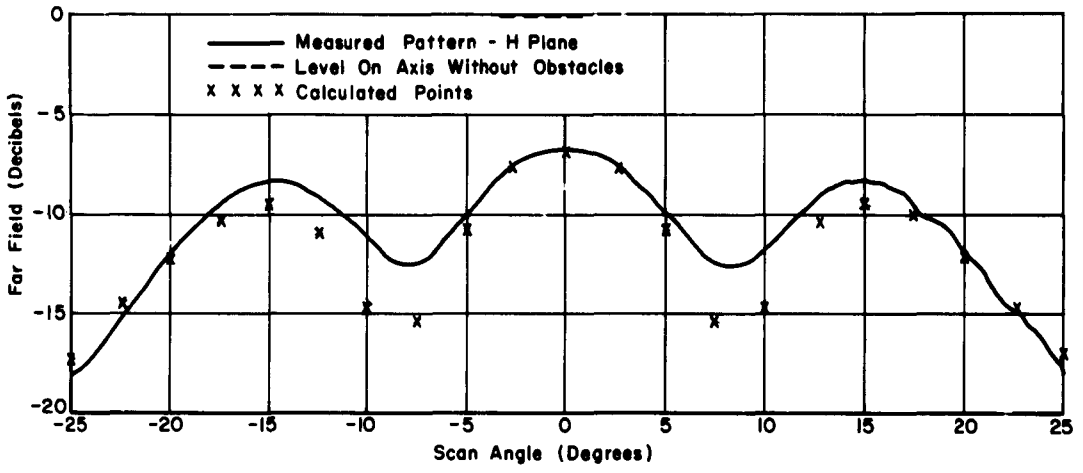

Fig. 17. The 5λ horn confronted by a 1.5λ cylinder at 6λ and dielectric sheet at 8λ.

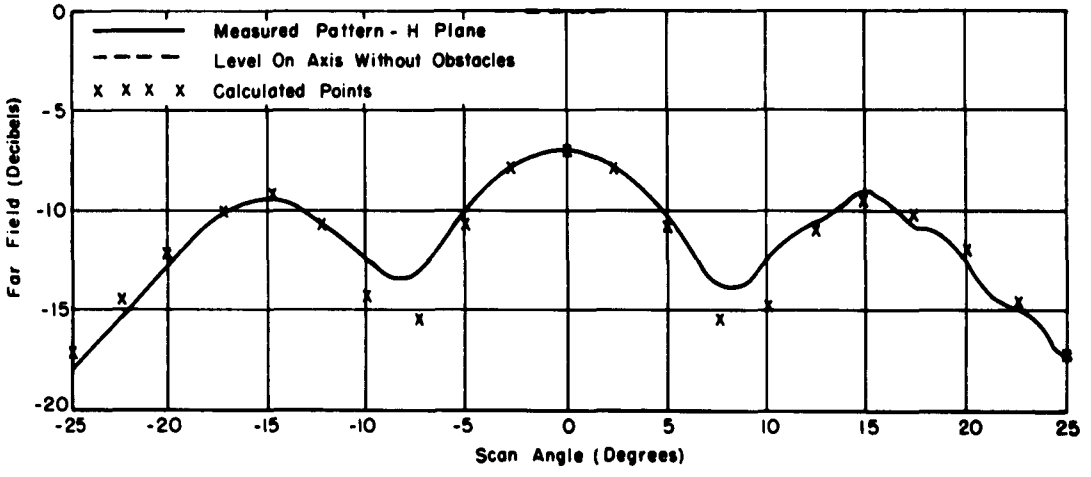

Fig. 18. The 5λ horn confronted by a 1.5λ cylinder at 6λ and dielectric sheet at 10.3λ.

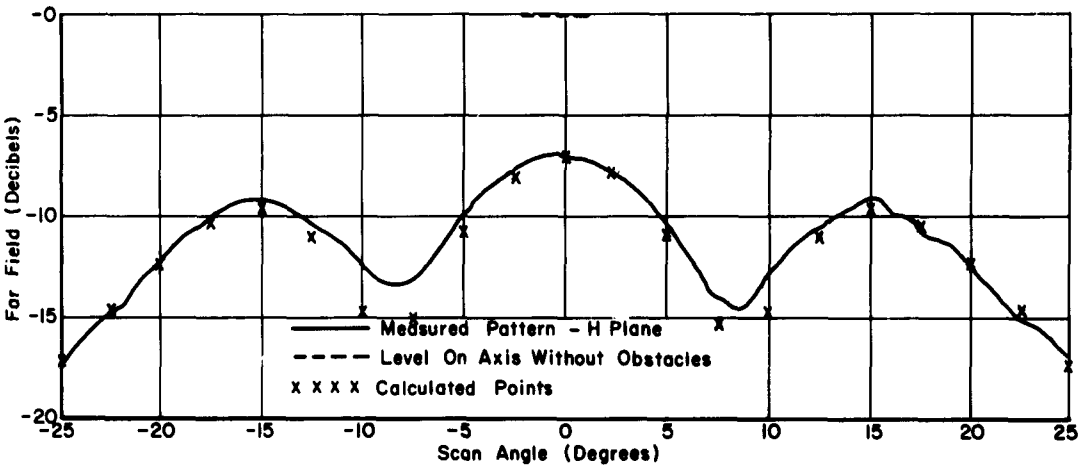

Fig. 19. The 5λ horn confronted by a 1.5λ cylinder at 6λ and dielectric sheet at 14λ.

A plane wave of unit amplitude incident upon the dielectric sheet is transmitted as a plane wave traveling in the same direction but with an amplitude equal to the plane-wave plane-sheet transmission coefficient, $T(\theta)$.[33] If such a plane wave should then encounter the cylinder it would be scattered according to Eqs. (40) through (55) with E_2 replaced by $T_\perp(\theta)E_2$. These scattered fields would then interact with the dielectric sheet and be reflected.

These last reflections were neglected in calculating the patterns shown in Figs. 15 thru 19. This approximate solution is applicable to pattern calculations of antennas confronted by structurally supported radomes. The agreement indicates that the higher order reflections can be neglected with some success, particularly when the sheet has a transmission coefficient of nearly unity.

3. A large ground plane antenna and a cylinder. The calculations made thus far have been based upon the assumption that the contributing portion of the antenna aperture fields are unaffected by the obstacle as discussed in Chapter II, Section C. This assumption is not always valid.

The antenna chosen to illustrate this point was an open ended waveguide in a large ground plane. A perfectly conducting cylinder ($d = 1.5\lambda$) six wavelengths from the aperture was oriented with its axis perpendicular to the H-plane. The measured H-plane pattern is shown in Fig. 20.

The H-plane pattern was computed assuming that the aperture fields were unaffected by the obstacle, Fig. 20. These calculations differed from the measurements appreciably because the cylinder induced large currents on the ground plane.

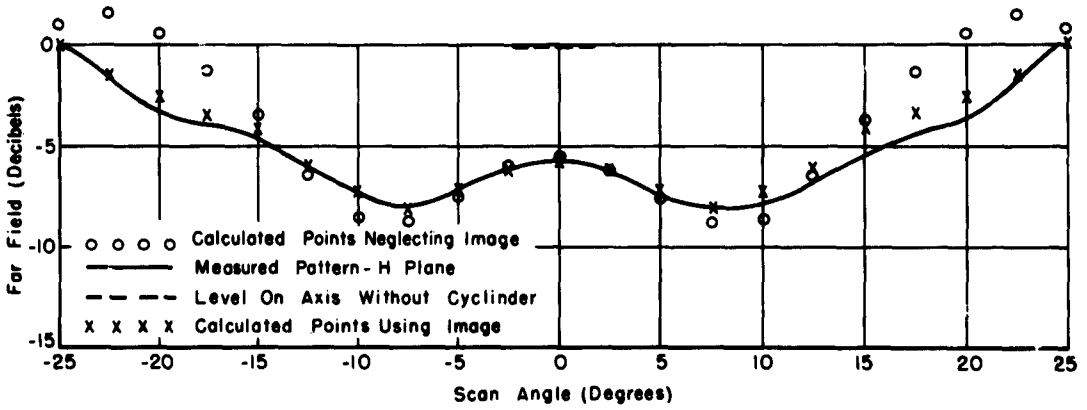

Fig. 20. Open ended waveguide in a large ground plane confronted by 1.5λ cylinder at a distance of 6λ.

In order to take into account this type of interaction, image theory was used. The plane wave scattered fields of the cylinder and its image were employed in Eq. (20) to calculate the antenna-cylinder pattern. Much better agreement was obtained (Fig. 20).

4. Antenna confronted by a pair of parallel cylinders. The last antenna-obstacle system treated consisted of an open ended waveguide and a pair of perfectly conducting parallel cylinders. The axes of the cylinders were perpendicular to the E plane of the antenna, and the plane of these cylinders was six wavelengths from the waveguide aperture. Each cylinder was of the same diameter ($d = 1.5\lambda$), and the cylinder axes were separated by slightly over four wavelengths ($s = 4.3\lambda$) as shown in Fig. 21.

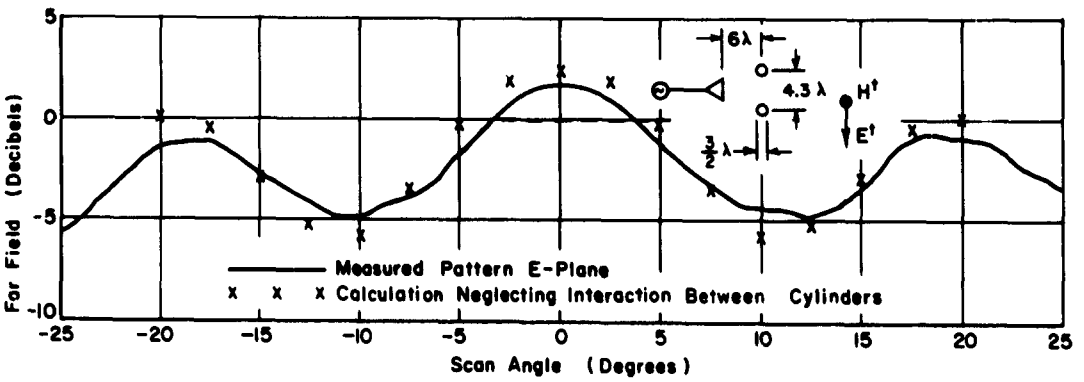

Fig. 21. Open ended waveguide-two parallel 1.5λ cylinders separated by 4.3λ.

The pattern of the system with one cylinder removed is shown in Fig. 22 along with calculations made by means of Eq. (20). The pattern of the system with the other cylinder in place and this cylinder removed would be a mirror image of Fig. 22 about the zero degrees scan axis.

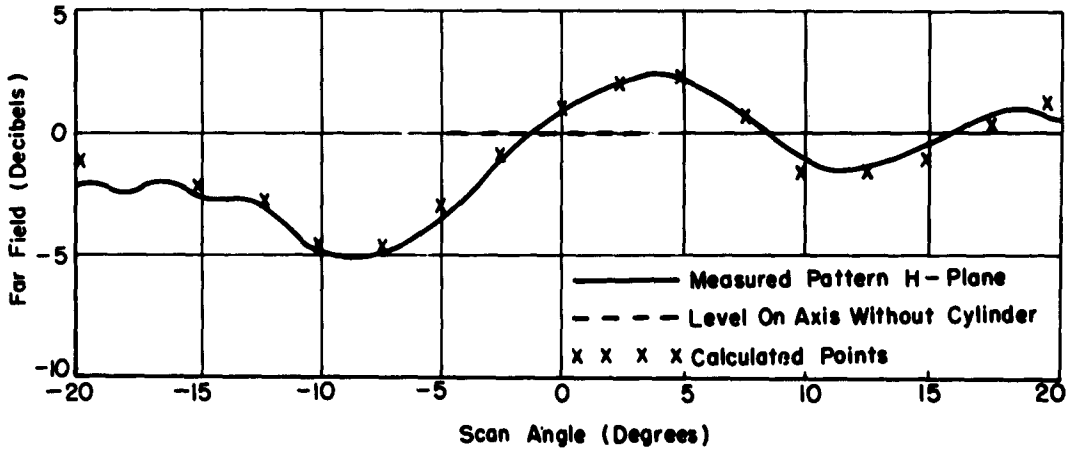

Fig. 22. Open ended waveguide-one cylinder off axis 20°.

In order to calculate the E-plane pattern of the system with both cylinders present by means of Eq. (20), the plane wave scattering by the pair of cylinders must be known. The success of neglecting

cylinder-sheet reflections in part two of this section suggested that a superposition of scattering by each cylinder alone would be a good zero-order approximation. The result of calculation and experiment is shown in Fig. 21. This approximation is seen to describe the general shape of the pattern but errors as great as two decibels are present. Thus a higher order approximation seems necessary.

CHAPTER V

CONCLUSIONS

In calculating the effect of an obstacle upon the performance of an antenna it is convenient to have an expression for the parameter of interest which can be programmed on a high-speed computer. The integral expressions for the electric field of an antenna-obstacle system Eqs. (20), (24) and (25) are of this type. These expressions are very general for they apply to any antenna-obstacle geometry and can be modified to obtain other pertinent parameters such as impedance, gain and boresight direction.

The possibility exists that the integrals can be evaluated in closed from but in the vast majority of instances the field quantities in the integrands will necessitate numerical integration. Often these quantities are known from measurement, design or as solutions to plane wave scattering problems. In these cases numerical integration yields a useful solution.

A choice of which expression to employ depends on the geometry of the problem and what is known about the antenna and obstacle. Most often the antenna aperture fields are known suggesting use of Eq. (20). Small scatterers, on the other hand, suggest an integration over the obstacle surface as in Eqs. (24) and (25).

Use of any of these expressions depends on a knowledge of either plane-wave scattering by the obstacle, Eqs. (20) and (24), or scattering of the antenna near-fields by the obstacle, Eq. (25). Since these quantities are known exactly for only a few obstacle geometries, approximate techniques are discussed. Several such techniques are discussed in Chapter III. A choice of which to employ depends upon the obstacle geometry. This is particularly true in the resonance region.

Use of Eq. (20) to calculate antenna-obstacle systems performance was highly successful in Chapter IV. The calculation of the patterns of an antenna confronted by a cylinder was completed employing approximate antenna aperture fields and the fields scattered from cylinders by a plane wave.

It was found that the asymptotic form of the plane-wave scattered fields could be used in making the calculations, for the cylinder sizes used and the antenna-to-cylinder spacings treated.

A very simple approximation yielded good results for plane sheet-cylinder combinations corresponding to structurally supported radomes, and some success was observed in treating

combinations of parallel cylinders. These results are applicable to the design and analysis of supported or sectioned radomes associated with ground-based antennas or antennas for hypersonic vehicles.

APPENDIX A

THE EXTERNAL BOUNDARY INTEGRAL

S_o, the external boundary of the volume V discussed in Chapter II and shown in Fig. 2 can be taken as a large sphere enclosing the smaller volumes V_1, V_2, and V_s. The existance of such a surface necessarily implies that the sources and scatterers are finite in extent and are finitely distributed within V.

Ballantine[34] discusses the integral and attempts to show that it equals zero on an infinite sphere.

The integral can be shown to be zero as a consequence of Sommerfeld's radiation condition as the sphere recedes to infinity.

A somewhat lengthy but straightforward proof is obtained by writing both sets of fields, $\underline{E}_1$, $\underline{H}_1$ and $\underline{E}_2$, $\underline{H}_2$, as expansions of outgoing waves such as the outgoing spherical wave functions. Such an expansion is valid on and exterior to S_o when it contains all sources and scatterers. Maxwell's equations and the orthogonality of the spherical wave functions on a sphere then cause the integral to vanish. The assumption of only outgoing waves depends upon the radiation condition, but the integration can be performed on a finite sphere rather than a sphere at infinity.

APPENDIX B

THE APERTURE FIELD APPROXIMATION

The free-space aperture fields of an antenna are perturbed when an obstacle is introduced because of multiple reflections between the obstacle and antenna structure.

Richmond [5] has shown that only outgoing fields contribute to integration on a surface enclosing the antenna. Therefore, only the reflections from the antenna need be considered as perturbations of the antenna aperture fields. In order to obtain some idea of the factors that effect the magnitude of these reflected fields a special case is treated.

Consider the antenna-obstacle system shown in Fig. 23. In order to simplify the analysis the antenna and obstacle are chosen to be infinite structures in the z direction with properties independent of z, furthermore the antenna fields are assumed polarized as shown in Fig. 23 ($\underline{H}$ transverse to $\hat{z}$). These restrictions reduce the problem to a two dimensional one.

The center of the antenna aperture coincides with the coordinate origin while the obstacle is located at (R_o, ϕ_o) .

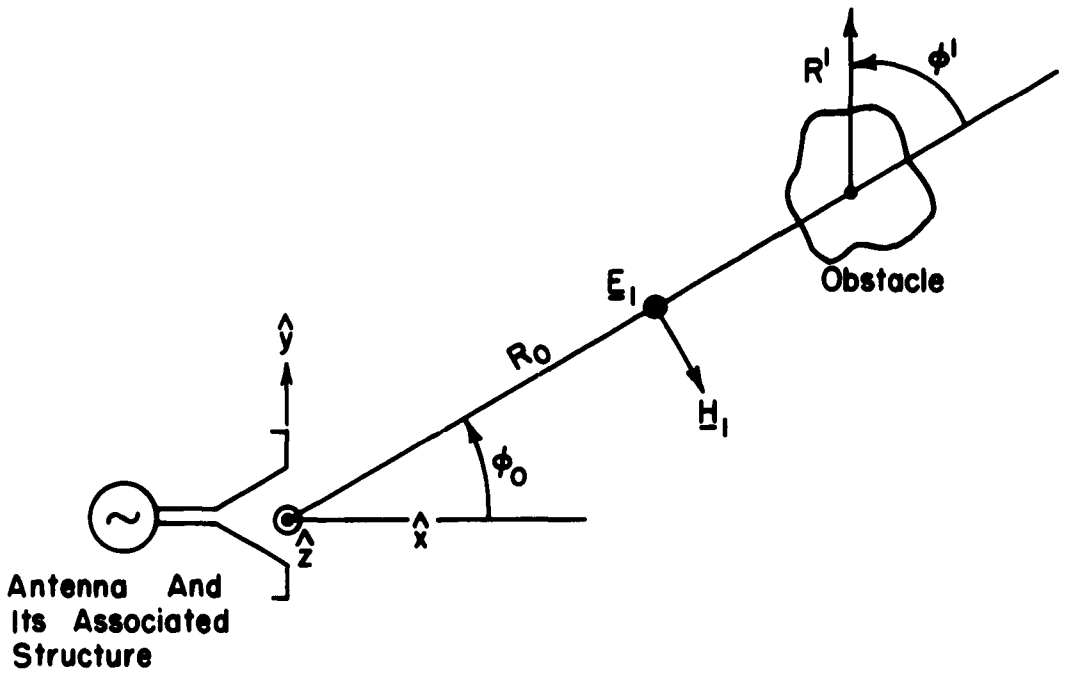

Fig. 23. The two dimensional antenna-obstacle system.

Consider the case for which R_o is so large that the obstacle lies in the far field of the antenna. The free-space antenna field, in the far field, can be written as

$$\underline{E}_1^o(R, \phi) = \hat{z}\, E_1^o(R, \phi) = \hat{z}\, \frac{e^{-jk_o R}}{\sqrt{R}}\, P(\phi) \quad . \tag{57}$$

When this field is incident upon the obstacle scattering occurs. At a great distance from the obstacle the scattered field, $\underline{E}_s^o$,

can be written as

$$\underline{E}_s^o (R', \phi') = \hat{z} \frac{e^{-jk_o R'}}{\sqrt{R'}} A(\phi') E_1^o (R_o, \phi_o) . \tag{58}$$

R' and ϕ' are cylindrical coordinates measured from the center of the obstacle, Fig. 23, and $A(\phi')$ is a complex reflection coefficient dependent upon the shape, orientation and constitutive parameters of the obstacle. Evaluating this field at the center of the antenna aperture, $R = 0$, yields

$$\underline{E}_s^o (R_o, \pi) = \hat{z} \frac{e^{-jk_o R_o}}{\sqrt{R_o}} A(\pi) E_1^o (R_o, \phi_o) . \tag{59}$$

$\underline{E}_s^o (R_o, \pi)$ encounters the antenna structure and is scattered. This scattered field, at the obstacle, can be written as

$$\underline{E}_1^1 (R_o, \phi_o) = \hat{z} E_1^1 (R_o, \phi_o) = \hat{z} \frac{e^{-jk_o R_o}}{\sqrt{R_o}} B(\phi_o) E_s^o (R_o, \pi), \tag{60}$$

where $B(\phi)$ is a complex reflection coefficient dependent upon the antenna structure, input impedance, and antenna-obstacle orientation.

This process of reflection and rereflection continues ad infinitum, and the field incident upon the antenna can be found by summing up the infinite number of reflections from the obstacle.

The total scattered field incident upon the antenna is

$$\underline{E}_s^t(R_o,\pi) = \underline{E}_s^o(R_o,\pi) + \underline{E}_s^1(R_o,\pi) + \underline{E}_s^2(R_o,\pi) \cdots , \tag{61}$$

so that

$$\underline{E}_s^t(R_o,\pi) = \hat{z}\,\frac{e^{-jk_oR_o}}{\sqrt{R_o}}\,A(\pi)\left(E_1^o(R_o,\pi) + E_1^1(R_o,\pi) + E_1^2(R_o,\pi)\cdots\right) \tag{62}$$

and

$$\underline{E}_s^t(R_o,\pi) = \hat{z}\,\frac{e^{-jk_oR_o}}{\sqrt{R_o}}\,A(\pi)\left(\frac{e^{-jk_oR_o}}{\sqrt{R_o}}\,P(\phi_o) + \frac{e^{-jk_oR_o}}{\sqrt{R_o}}\,P(\phi_o)\,A(\pi)\,B(\phi_o)\,\frac{e^{-jk_o2R_o}}{R_o} + \frac{e^{-jk_oR_o}}{\sqrt{R_o}}\,P(\phi_o)\,A^2(\pi)B^2(\phi_o)\,\frac{e^{-jk_o4R_o}}{R_o^2}\cdots\right) . \tag{63}$$

This expression is a geometric series which can be summed when

$$\left|A(\pi)\,B(\phi_o)\,\frac{e^{-jk_o2R_o}}{R_o}\right| < 1 , \tag{64}$$

which is true for large R_o. Thus, the total field incident upon the antenna is

$$\underline{E}_s^t(R_o,\pi) = \hat{z}\,\frac{\dfrac{e^{-jk_o2R_o}}{R_o}\,A(\pi)\,P(\phi_o)}{1 - \dfrac{A(\pi)\,B(\phi_o)\,e^{-j2k_oR_o}}{R_o}} ; \tag{65}$$

Eq. (65) can be rewritten as

$$\underline{E}_s^t(R_o, \pi) = \hat{z}\, \frac{A(\pi)\, P(\phi_o)\, e^{-jk_o 2R_o}}{R_o - A(\pi)\, B(\phi_o)\, e^{-j2k_o R_o}} \quad . \tag{66}$$

A similar summation yields the magnetic field incident upon the antenna,

$$\underline{H}_s^t(R_o, \pi) = \frac{(-\hat{R} \times \hat{z})}{Z_o}\, \frac{A(\pi)\, P(\phi_o)\, e^{-j2k_o R_o}}{R_o - A(\pi)\, B(\phi_o)\, e^{-j2k_o R_o}} \quad . \tag{67}$$

When these fields are incident upon the antenna they are reflected from the metal and dielectric positions of the structure as well as the antenna terminals. At a great distance, the field scattered from the antenna can be written as

$$\begin{aligned} \underline{E}_1^t(R, \phi) &= \hat{z}\, \frac{B(\phi)\, e^{-jk_o R}}{\sqrt{R}}\, E_s^t(R_o, \pi) \\ &= \hat{z}\, \frac{A(\pi)\, P(\phi_o)\, B(\phi)\, e^{-jk_o(2R_o + R)}}{\sqrt{R}\, (R_o - A(\pi)\, B(\phi_o)\, \epsilon^{-j2k_o R_o})} \quad , \end{aligned} \tag{68}$$

where $B(\phi)$ depends upon the antenna structure and its orientation with respect to the obstacle.

The total field incident upon the obstacle is

$$\underline{E}_1 (R_o, \phi_o) = \underline{E}_1^o (R_o, \phi_o) + \underline{E}_1^t (R_o, \phi_o) \cdot \tag{69}$$

Equation (69) can be written out in detail as

$$\underline{E}_1 (R_o, \phi_o) = \hat{z} \frac{P(\phi_o) e^{-jk_o R_o}}{\sqrt{R_o}} \left(1 + \frac{A(\pi) B(\phi_o) e^{-j2k_o R_o}}{R_o - A(\pi) B(\phi_o) e^{-j2k_o R_o}} \right) \tag{70}$$

and

$$\underline{E}_1 (R_o, \phi_o) = \hat{z} \frac{P(\phi_o) e^{-jk_o R_o} \sqrt{R_o}}{(R_o - A(\pi) B(\phi_o) e^{-j2k_o R_o})} \cdot \tag{71}$$

At great distances the total fields scattered from the obstacle can be written as

$$\underline{E}_s^t (R', \phi') = \hat{z} \frac{A(\phi') e^{-jk_o R'}}{\sqrt{R'}} E_1 (R_o, \phi_o) \tag{72}$$

$$= \hat{z} \frac{A(\phi') P(\phi_o) \sqrt{R_o} e^{-jk_o (R_o + R')}}{\sqrt{R'} (R_o - A(\pi) B(\phi_o) e^{-j2k_o R_o})}$$

and

$$\underline{H}_s^t (R', \phi') = \frac{(\hat{R}' \times \hat{z}) A(\phi') e^{-jk_o R'}}{Z_o \sqrt{R'}} E_1 (R_o, \phi_o) \cdot \tag{73}$$

Finally, the electric field of the antenna-obstacle system can be written as the sum of the free-space antenna field, the total field scattered from the obstacle, and the total field scattered from the antenna. Thus

$$\underline{E}_1(R, \phi) = \underline{E}_1^o(R, \phi) + \underline{E}_1^t(R, \phi) + \underline{E}_s^t(R', \phi') \tag{74}$$

and

$$\underline{E}_1(R, \phi) = \hat{z}\ \left[E_1^o(R, \phi) + E_1^t(R, \phi) + \frac{A(\phi')\ e^{-jk_o R'}}{\sqrt{R'}}\right.$$

$$\left.(E_1^o(R_o, \phi_o) + E_1^t(R_o, \phi_o))\right] . \tag{75}$$

An approximate solution of this antenna-obstacle problem which neglects the fields scattered from the antenna structure (i.e., it is assumed that $E_1^t = 0$) can be written as

$$\underline{E}_1(R, \phi) = \hat{z}\ \left[E_1^o(R, \phi) + \frac{A(\phi')\ e^{-jk_o R'}}{\sqrt{R'}}\ E_1^o(R_o, \phi_o)\right] . \tag{76}$$

The error, $W(R, \phi)$, due to this approximation is given by the difference of Eq.(75) and (76). Thus

$$W(R, \phi) = \hat{z}\ \left[E_1^t(R, \phi) + \frac{A(\phi')\ e^{-jk_o R'}}{\sqrt{R'}}\ E_1^t(R_o, \phi_o)\right] , \tag{77}$$

and Eq. (68) yields

$$(78) \qquad W(R, \phi) = \hat{z} \frac{A(\pi)\, P(\phi_o)\, e^{-j2k_o R_o}}{[R_o - A(\pi)\, B(\phi_o)\, e^{-j2k_o R_o}]} \left(\frac{B(\phi)\, e^{-jk_o R}}{\sqrt{R}} + \frac{B(\phi_o)\, A(\phi')\, e^{-jk_o (R' + R_o)}}{\sqrt{R_o}\ \sqrt{R}} \right),$$

when the point of observation, (R, ϕ), is far from both the antenna and obstacle.

Examination of this expression for the error introduced by approximating the aperture fields by the free-space aperture fields leads to the following conclusions.

1. The error depends upon the magnitude of the reflection coefficient of the obstacle in a direction back toward the antenna, $A(\pi)$. The smaller this coefficient— the smaller the error.
2. The error is directly proportional to the relative illumination of the obstacle by the antenna, $P(\phi_o)$. The angular position of the obstacle greatly affects the accuracy of the aperture field assumption.

3. The error depends upon the separation of the antenna and obstacle, R_o. For the case considered, R_o large, the error is inversely proportional to the separation and rapidly becomes very small in comparison with the approximate solution, Eq. (77).

4. The error depends upon the reflection coefficient of the antenna, $B(\phi)$ and $B(\phi_o)$. In some instances the major contribution to antenna scattering is a reflection at the antenna terminals. In this case

(79) $$B(\phi) = CP(\phi) ,$$

where C is a constant dependent upon the amount of mismatch at the antenna terminals. In other cases (e.g., antenna mounted in a large ground plane) $B(\phi)$ and $P(\phi)$ are vastly different functions.

The treatment of this two dimensional problem serves to indicate the type of approximation involved in employing the free-space aperture fields of an antenna. Each antenna-obstacle system encountered should be analyzed in terms of the above factors. Such an analysis will often indicate when the approximation is not expected to be accurate and why.

The analysis can be extended to the case of arbitrary polarization by first considering TE fields and the analogous reflection coefficients, $B'(\phi)$ and $A'(\phi')$. Arbitrary polarizations are treated as a superposition of TE and TM waves so that the reflection coefficients become two by two matrices. Obstacles in the near field of antennas further complicate the problem, for the incident fields cannot be treated as plane waves and the use of reflection coefficients such as $B(\phi)$ and $A(\phi')$ is no longer justifiable. In this case the use of an infinite scattering matrix that relates the field scattered from a body to the incident field is appropriate. In the two dimensional case the scattering matrices should be referred to cylindrical coordinate systems.

Treatment of three dimensional antenna-obstacle geometries is complicated by the addition of another variable, but closely follows the two dimensional case. In the far field two by two matrix reflection coefficients can be defined that depend upon the shape, orientation, and constitutive parameters of the scatterer while in the near field infinite scattering matrices should be employed.

APPENDIX C

ELIMINATION OF THE INTEGRAL OVER S_s

In formulating Eq. (19) the environment of antenna 2 was left arbitrary within the volume V_s. By an appropriate choice of this environment Eq. (19) is simplified.

Case 1. The scatterer is a perfect conductor.

The surface integral over S_s from Eq. (20) can be rewritten as

$$(80) \qquad \int_{S_s} (\underline{E}_1 \times \underline{H}_2 - \underline{E}_2 \times \underline{H}_1) \cdot \hat{n}\, dS = \int_{S_s} (\hat{n} \times \underline{E}_1 \cdot \underline{H}_2 - \hat{n} \times \underline{E}_2 \cdot \underline{H}_1)\, dS \ .$$

The surface S_s is now chosen to coincide with the perfectly conducting surface. The necessary boundary condition on $\underline{E}_1$ is that $\hat{n} \times \underline{E}_1 = 0$ on S_s so that

$$(81) \qquad \int_{S_s} (\underline{E}_1 \times \underline{H}_2 - \underline{E}_2 \times \underline{H}_1) \cdot \hat{n}\, dS = - \int_{S_s} (\hat{n} \times \underline{E}_2) \cdot \underline{H}_1\, dS \ .$$

Furthermore, if the perfect conductor is also a part of the environment of antenna 2 then $\hat{n} \times \underline{E}_2 = 0$ on S_s and

$$(82) \qquad \int_{S_s} (\underline{E}_1 \times \underline{H}_2 - \underline{E}_2 \times \underline{H}_1) \cdot \hat{n}\, dS = 0$$

so that Eq. (19) becomes

$$(83) \qquad \int_{S_1} (\underline{E}_1 \times \underline{H}_2 - \underline{E}_2 \times \underline{H}_1) \cdot \hat{n}\, dS = \underline{E}_1 (x_o, y_o, z_o) \cdot \hat{\ell}_2\, I_2 \,.$$

Case 2. The scatterer is isotropic and described by the complex scalar quantities $\mu_1 (x, y, z)$ and $\epsilon_1 (x, y, z)$.

The surface integral over S_s can be rewritten as

$$(84) \qquad \int_{S_s} (\underline{E}_1 \times \underline{H}_2 - \underline{E}_2 \times \underline{H}_1) \cdot \hat{n}\, dS = \int_{V_s} \nabla \cdot (\underline{E}_1 \times \underline{H}_2 - \underline{E}_2 \times \underline{H}_1)\, dV$$

and by using a vector identity

$$(85) \qquad \int_{S_s} (\underline{E}_1 \times \underline{H}_2 - \underline{E}_2 \times \underline{H}_1) \cdot \hat{n}\, dS =$$

$$= \int_{V_s} (\underline{H}_2 \cdot \nabla \times \underline{E}_1 - \underline{E}_1 \cdot \nabla \times \underline{H}_2 + \underline{E}_2 \cdot \nabla \times \underline{H}_1 - \underline{H}_1 \cdot \nabla \times \underline{E}_2)\, dV \,.$$

Inside V_s, which is source free,

$$(86) \qquad \nabla \times \underline{E}_1 = -j\omega\, \mu_1 (x, y, z)\, \underline{H}_1 \,,$$

$$(87) \qquad \nabla \times \underline{H}_1 = j\omega\, \epsilon_1 (x, y, z)\, \underline{E}_1 \,,$$

and

$$\nabla \times \underline{E}_2 = -j\omega \mu_2 (x, y, z)\, \underline{H}_2 \quad , \tag{88}$$

$$\nabla \times \underline{H}_2 = j\omega\, \epsilon_2 (x, y, z)\, \underline{E}_2 \quad , \tag{89}$$

so that

$$\int_{S_s} (\underline{E}_1 \times \underline{H}_2 - \underline{E}_2 \times \underline{H}_1) \cdot \hat{n}\, dS = \int_{V_s} [\underline{H}_2 \cdot (-j\omega\mu_1 \underline{H}_1) - \underline{E}_1 \cdot (j\omega\epsilon_2 \underline{E}_2) + \underline{E}_2 \cdot (j\omega \epsilon_1 \underline{E}_1) - \underline{H}_1 \cdot (-j\omega\mu_2 \underline{H}_2)]\, dV \tag{90}$$

or

$$\int_{S_s} (\underline{E}_1 \times \underline{H}_2 - \underline{E}_2 \times \underline{H}_1) \cdot \hat{n}\, dS = \int_{V_s} -j\omega\, [\underline{H}_2 \cdot \underline{H}_1 (\mu_1 - \mu_2) + \underline{E}_1 \cdot \underline{E}_2 (\epsilon_2 - \epsilon_1)]\, dV \, . \tag{91}$$

By choosing $\mu_2 = \mu_1$ and $\epsilon_2 = \epsilon_1$ at all points within V_s the integrand vanishes identically so that

$$\int_{S_s} (\underline{E}_1 \times \underline{H}_2 - \underline{E}_2 \times \underline{H}_1) \cdot \hat{n}\, dS = 0 \tag{92}$$

and Eq. (19) again reduces to Eq. (83).

The surface integration on S_s thus can be eliminated by choosing the same environment for antenna 2 as for antenna 1 outside of the source regions S_1 and S_2 .

BIBLIOGRAPHY

1. Richmond, J.H., "A Reaction Theorem and Its Application to Antenna Impedance Calculations," Report 1180-1, 16 August 1960, Antenna Laboratory, The Ohio State University Research Foundation; prepared under Contract AF 33(616)-7614, Air Research and Development Command, Wright Air Development Center, Wright-Patterson Air Force Base, Ohio.
2. Richmond, J.H., "On the Theory of Scattering by Dielectric and Metal Objects," Report 786-3, 1 April 1958, Antenna Laboratory, The Ohio State University Research Foundation; prepared under Contract AF 33(616)-5410, Air Research and Development Command, Wright Air Development Center, Wright-Patterson Air Force Base, Ohio.
3. Rumsey, V.H., "Reaction Concept in Electromagnetic Theory," Physical Review, Vol. 94, No. 6, pp. 1483-91, 15 June 1954.
4. Ballantine, S., "Reciprocity in Electromagnetic, Mechanical, Acoustical, and Interconnected Systems," Proc. I.R.E., Vol. 17, p. 929, June 1929
5. Richmond, J.H., Report 786-3, op.cit., p. 33.

6. Rayleigh, Lord, "On the Incidence of Aerial and Electric Waves Upon Small Obstacles in the Form of Ellipsoids or Elliptic Cylinders, and on the Passage of Electric Waves Through a Circular Aperture in a Conducting Screen," The Phil. Mag., 44, pp. 28-52, July 1897.

7. Cohen, M.H., "Application of the Reaction Concept to Scattering Problems," I.R.E., PGAP, Vol. AP-3, p. 194, October 1955.

8. Baechle, J.R., Richmond, J.H., and Stickler, D.C., "Antenna Pattern Distortion by a Wedge-Shaped Radome," Report 655-2, 1 March 1956, Antenna Laboratory, The Ohio State University Research Foundation; prepared under Contract AF 33(616)-3212, Air Research and Development Command, Wright Air Development Center, Wright-Patterson Air Force Base, Ohio.

9. Richmond, J.H., "Electromagnetic Transmission Through Dielectric Sheets," Report 531-12, 30 September 1955, Antenna Laboratory, The Ohio State University Research Foundation; prepared under Contract AF 33(616)-277, Air Research and Development Command, Wright Air Development Center, Wright-Patterson Air Force Base, Ohio.

10. Richmond, J.H., "The WKB Solution for Transmission Through Inhomogeneous Plane Layers," Report 1180-6, 15 September 1961, Antenna Laboratory, The Ohio State University Research Foundation; prepared under Contract AF 33(616)-7614, Aeronautical Systems Division, Air Force Systems Command, Wright-Patterson Air Force Base, Ohio.

11. Richmond, J.H., "Transmission Through Inhomogeneous Plane Layers," Report 1180-4, 15 July 1961, Antenna Laboratory, The Ohio State University Research Foundation; prepared under Contract AF 33(616)-7614, Air Research and Development Command, Wright Air Development Center, Wright-Patterson Air Force Base, Ohio.

12. Schelkunoff, S.A., Electromagnetic Waves, D.Van Nostrand Co., Inc., New York, pp. 158-159, 1943.

13. Harrington, R.F., "On Scattering by Large Conducting Lodies," I.R.E., PGAP, Vol. AP-7, pp. 150-153, April 1959.

14. Stratton, J.A., Electromagnetic Theory, McGraw-Hill Book Co., Inc., New York, pp. 10-12, 1941.

15. Morse, P.M. and Feshbach, H., Methods of Theoretical Physics, McGraw-Hill Book Co., Inc., New York, Vol. I, pp. 494-522, 1953.

16. Morse, P.M. and Feshbach, H., op. cit., pp. 1387-1398.

17. Morse, P.M. and Feshbach, H., op. cit., pp. 1428-1430.

18. Kantorovich, L.V. and Krylov, V.I., Approximate Methods of Higher Analysis, Interscience Publishers, Inc., New York, 1958.

19. Kennaugh, E.M., "Multipole Field Expansions and Their Use in Approximate Solutions of Electromagnetic Scattering Problems," Report 827-5, 1 November 1959, Antenna Laboratory, The Ohio State University Research Foundation; prepared under Contract AF 19(604)-3501, Air Force Cambridge Research Center, Cambridge, Massachusetts.

20. Rumsey, V.H., op. cit.

21. Fock, V.A., "Distributions of Currents Induced by a Plane Wave on the Surface of a Conductor," J.Phys. (USSR), Vol. 10, 1946.

22. Goodrich, R.F., "Studies in Radar Cross Section. XXVI, Fock Theory," Scientific Report No. 3, University of Michigan Research Institute, July 1958.

23. Wetzel, L., "High-Frequency Current Distributions on Conducting Obstacles," Scientific Report No. 10, Cruft Laboratory, Harvard University, May 1957.

24. Wu, Tai Tsun, "High Frequency Scattering," Technical Report No. 232, Cruft Laboratory, Harvard University, 25 May 1956.

25. Wetzel, L., op. cit.

26. King, R.W.P. and Wu, T.T., The Scattering and Diffraction of Waves, Harvard University Press, Cambridge, Massachusetts, 1959.

27. Keller, J.B., "The Geometrical Theory of Diffraction," Research Report No. EM-115, Institute of Mathematical Sciences, New York University, New York, July 1958.

28. Thomas, D., "Approximations for Backscatter from a Dielectric Sphere," Report 1116-14, December 1961, Antenna Laboratory, The Ohio State University; prepared under Contract AF 19(604)-7270, Air Force Cambridge Research Laboratories, Cambridge, Massachusetts.

29. Charlton, T.E., "The Quadripod Space Frame and Antenna System Performance," Report 1180-2, 1 March 1961, Antenna Laboratory, The Ohio State University; prepared under Contract AF 33(616)-7614, Air Research and Development Command, Wright Air Development Center, Wright-Patterson Air Force Base, Ohio.

30. Morse, P.M. and Feshbach, H., op. cit., p. 1863.

31. Frank, P. and Von Mises, R., Die Differentialglichungen und Integralgleichungen der Mechanik und Physik, Mary S. Rosenberg, New York, p. 869, 1943.

32. Tang, Charles C.H., "Backscattering from Dielectric-Coated Infinite Cylindrical Obstacles," Journal of Applied Physics, May 1957.

33. Tice, Thomas E., (Editor-in-chief), "Techniques for Airborne Radome Design," WADC Technical Report 57-67, September 1957. The McGraw-Hill Book Co., Inc., Technical Writing Service; prepared under Contract AF 33(616)-3279, Air Research and Development Command, Wright Air Development Center, Wright-Patterson Air Force Base, Ohio, pp. 27-47.

34. Ballantine, S., op. cit.

35. Richmond, J.H., "A Reaction Theorem and Its Application to Antenna Impedance Calculations," Report 1180-1, 1 November 1960, Antenna Laboratory, The Ohio State University Research Foundation; prepared under Contract AF 33(616)-7614, Wright Air Development Division, Wright-Patterson Air Force Base, Ohio.

PROJECT 1180
REPORTS DISTRIBUTION LIST
CONTRACT NO. AF 33(616)7614

Copies	Destination
10	ASTIA, Arlington Hall Station, Arlington 12, Virginia
2	ASD (ASRNRE-4) WPAFB, Ohio
1	ASD (ASRNOP) WPAFB, Ohio
1	Director, USAF Project Rand, Via: SBAMA, AMC, Liaison Office, The Rand Corporation, 1700 Main Street, Santa Monica, California
3	AFCRL (CRRD), Laurence G. Hanscom Field, Bedford, Mass.
1	Air Force Development Field Representative, Code 1072, Naval Research Laboratory, Washington 25, D.C.
1	Chief, Bureau of Aeronautics, Avionics Division, Material Coordination Unit, Department of the Navy, Washington 25, D.C.
1	Chief, Bureau of Ships, Code 816-E, Department of the Navy, Washington 25, D.C.
1	Director, Surveillance Department, Evans Area; Attn: Technical Document Center, Belmar, New Jersey.
2	Commanding General, Redstone Arsenal, ATTN: Technical Library-EC, Redstone Arsenal, Alabama
1	National Bureau of Standards, Electricity and Electronics Division, Engineering Electronics Section, Attn: Mr. Gustave Shapiro, Washington 25, D.C.
1	Advisory Group on Electron Tubes, Attn: H.W. Serig, 346 Broadway, 8th Floor, New York 13, New York.
1	Naval Air Development Center Attn: Jerry Guarini (EL-72) Johnsville, Pennsylvania
1	Bureau of Weapons Attn: C.F. Bersch (RRMA-34) Department of the Navy Washington 25, D.C.